The Ferrous Regeneration Process for Use in Alternate Anode Reaction Technology in Copper Hydrometallurgy

Emily Allyn Sarver

Virginia Polytechnic Institute and State University

Master of Science
in
Mining and Minerals Engineering

Gregory Adel, Chair
Maurice Fuerstenau
Gerald Luttrell
Thomas Novak

July 26, 2005
Blacksburg, Virginia

Keywords: AART, ferric reduction, sulfur dioxide oxidation, activated carbon, mass transfer kinetics

The Ferrous Regeneration Process for Use in Alternate Anode Reaction Technology in Copper Hydrometallurgy

Emily Allyn Sarver

Abstract

The Fe(II) regeneration process is an important aspect of Alternate Anode Reaction Technology (AART) using Fe(II)/Fe(III)-SO_2 reactions for copper hydrometallurgy; however little has been done to study it specifically. The process regenerates Fe(II) via Fe(III) reduction by $SO_{2(aq)}$, catalyzed by activated carbon particles. To better understand and improve the process, two studies have been conducted with respect to variable factors and their affects on the regeneration.

A study of fundamental kinetics confirms that the regeneration reaction is mass transfer-controlled, requiring adsorption of reactants onto the catalyst surface for reaction. The reaction rate is limited by the diffusivity of Fe(III). Initial Fe(III) concentration and carbon particle size are determined to be the most influential factors on the rate under the condition studied. Furthermore, it is observed that flow rate may inhibit the reaction by reducing ion diffusivity. The experimentally validated rate expression for the regeneration is below, where the Fe(III) diffusivity is 1.1×10^{-7} cm^2/s.

$$\frac{dFe^{2+}}{dt} = \frac{6M}{\rho d V}\left[\frac{2D_f}{d} + 0.6\frac{V_t^{1/2} D_f^{2/3}}{d^{1/2} v^{1/6}}\right][C_{Fe^{3+}}]$$

An optimization problem is also developed and solved for the process, constrained by the requirement that negligible SO_2 could be present in the process effluent. Before optimization, a relationship is developed between regeneration rate and variable factors. Again, carbon size and initial Fe(III) are the most influential factors on the regeneration rate, related to it linearly; temperature is significant with a squared relationship to the rate; initial SO_2 is insignificant. Optimal conditions are found with minimum carbon particle size, maximum initial Fe(III) concentration, and moderate temperature.

Acknowledgements

The author would like to extend her sincere gratitude to Dr. Greg Adel for all of his time, efforts, advice and his unwavering support, without which this work, and many other goals, could not have been completed. He is one of a kind in his profession and an exemplary role model.

Much appreciation is owed to the Phelps Dodge Process Technology Center for allowing such a valuable opportunity as to work on this project. To Scot Sandoval and many friends at the SX/EW Test Facility, the author would like to give special thanks. Their talents made this work possible, and their generosity, patience and humor made it a joy.

Many thanks are also offered to Dr. Maury Fuerstenau, with whom it was truly a wonderful experience to work. His knowledge and guidance were invaluable to this work, and his good nature was invaluable to the process.

Finally, the author would like to express her gratefulness to her family. They taught her to dream, aspire, persevere, and succeed.

Table of Contents

List of Figures

List of Tables

Chapter 1: Introduction

The Copper Industry

Copper has been used for millenniums due to its unique properties and, in fact, is currently the third most used metal, after iron and aluminum. In addition to being malleable and ductile, copper forms favorable alloys because it is corrosion resistant, biostatic and easily cast, and is an exceptional electrical and thermal conductor. Today, copper is nearly exclusively exploited for its conductivity and resistance to corrosion, and the rapid progression of construction and technology maintains a high demand for the metal. In 2003, about 17 million metric tons of copper were produced to supply the significantly growing global demand (ICGS, 2003).

Like in all commodity markets, as demand has grown so have copper prices due to depleted stocks and the fact that increased production inherently lags demand. In April 2005, the copper spot price reached a high of $1.54 per pound, up from $0.65 just two years earlier (LME, 2005). High prices are good for producers – so good that many have re-opened existing capacities or brought new capacities online to take advantage of the supply deficit – but how long will they last?

Over the next 10 to 15 years, worldwide copper demand is expected to increase with growing economies (Demler, 2005). This is especially of interest when considering the major copper producing and consuming nations and their respective economies. For example, Chile accounts for nearly 35% of global production and only about 1% of consumption, the U.S. nearly balances its production and consumption at 18% and 16% respectively, and China accounts for only 5% of production and over 17% of consumption (ICGS, 2003). Of the three, the Chinese economy (and demand for copper) stands out with enormous recent growth, a trend which is expected to continue for quite some time.

While copper supplies are also expected to increase, causing the market to cycle to balance supply and demand, increasing production costs will likely shift the average cycle

price upwards. If prices tend to remain elevated with production costs, a real opportunity is presented for low-cost producers; increased profits are available for corporate expansion and for investments, and investments in technological improvements and development will perpetuate growing profit margins.

Hydrometallurgy: Past, Present and Future

Progression in Copper Processing

Hydrometallurgy was integrated into commercial copper production in the late 1970's as a means of processing additional ore types at lower costs than pyrometallurgy. The processing method can be applied to both oxide and oxidized sulfide ores or wastes, unlike pyrometallurgy, which only be applied to sulfide ores.

The processing costs of hydrometallurgy are also more attractive than those of its counterpart because of the difference in overall power consumption. Hydrometallurgy has an associated power requirement of about 10 to 35MJ/kg of copper produced; the wide variation depends largely on whether the source is previous waste or newly mined ore. Comparatively, pyrometallurgy requires about 65MJ/kg, utilizing much of the power for the energy intensive comminution needed to reduce particles to floatable sizes (Dresher, 2001).

Additionally, hydrometallurgy is considered relatively neutral with respect to environmental effects, generating air emissions only from power consumption and wastes that can be safely disposed in excavated areas. Due to its many benefits, hydrometallurgical processing now accounts for over 21% of global copper production, mostly in Chile and the U.S., the two largest producing countries, and continues to grow rapidly.

The General Hydrometallurgical Process

Copper hydrometallurgy is typically considered to encompass three major phases: leaching, solvent extraction (SX) and electrowinning (EW). Leaching refers to the dissolution and extraction of copper-bearing minerals from coarsely crushed copper ore using acidic solutions. Following leaching, the solution containing extracted copper minerals is collected and sent to the SX phase.

During SX, aqueous leach solution is mixed with an organic phase specifically developed to remove the dissolved copper, leaving most of the dissolved impurities behind. The copper-deficient leach solution is recycled back to the leaching phase; the copper-rich organic is treated with another chemical called a stripper, which transfers the copper minerals from the organic to an aqueous phase. The stripped organic is then recycled back to the SX phase, and the copper-rich aqueous electrolyte is sent to the EW phase.

EW refers to the process of plating metallic copper from copper electrolyte, in which it is present as copper (II) sulfate ($CuSO_4$). This is done by filling large tanks that have an alternating series of anodes and cathodes with the electrolyte and passing current. The electrical potential provided drives an oxidation reaction at the anodes that is balanced by a reduction reaction at the cathodes, onto which the copper plates. The conventional reactions, which are discussed in further detail below, are water oxidation and copper reduction, whereby divalent copper is reduced to the neutral metallic species.

Conventional Electrowinning vs. Alternate Anode Reaction Technology

Two main areas of concern in conventional copper EW are relatively high power consumption and acid misting, both of which are associated with the oxidation of water as the anode reaction. The EW power requirement, mostly due to the cell voltage requirement, accounts for 30 to 50% of the total requirement for hydrometallurgical processing, which can be problematic from a financial perspective and also with respect to growing concern for the environment. Acid misting is a product of oxygen gas (O_2) generation at the anode, which causes a hazardous and uncomfortable environment for those working in EW tank houses, as well as corrosive conditions for structures and equipment.

To address both of the above issues, alternate anode reaction technology (AART) has been suggested as a possible solution. AART refers to changing the conventional anode reaction, preferably to one that has a considerably lower equilibrium potential, such that power consumption is reduced, and which also does not produce a gas that causes acid misting. For copper EW, a ferrous [Fe(II)] to ferric [Fe(III)] iron oxidation reaction appears

quite feasible as an alternate anode reaction for several reasons (Sandoval and Dolinar, 1996):

- it has a significantly smaller equilibrium potential;
- iron is already present in commercial electrolytes (due to its abundance in most copper ores); and
- oxidized Fe(II) may be regenerated by reducing Fe(III) such that electrolyte solutions can remain recyclable – the proposed reducing agent is sulfur dioxide (SO_2), possibly from burners at nearby smelting operations due to its availability and low cost.

A comparison of the conventional and proposed AART reactions is given in Table 1.1, highlighting the difference between the anode and overall equilibrium potentials.

Table 1.1 – Conventional and Proposed AART Electrode Reactions

	Conventional		AART	
	Reaction	Equilibrium Potential	Reaction	Equilibrium Potential
Oxidation half-reaction (anode):	$H_2O \rightarrow \frac{1}{2}O_2 + 2H^+ + 2e^-$	$E_{ox}^{\ 0} = -1.229V$	$2 \times (Fe^{2+} \rightarrow Fe^{3+} + e^-)$	$E_{ox}^{\ 0} = -0.770V$
Reduction half-reaction (cathode):	$CuSO_4 + 2e^- \rightarrow SO_4^{2-} + Cu$	$E_{red}^{\ 0} = 0.345V$	$CuSO_4 + 2e^- \rightarrow SO_4^{2-} + Cu$	$E_{red}^{\ 0} = 0.345V$
Balanced reaction (total):	$CuSO_4 + H_2O \rightarrow \frac{1}{2}O_2 + H_2SO_4 + Cu$	$E_{total}^{\ 0} = -0.884V$	$CuSO_4 + 2Fe^{2+} \rightarrow 2Fe^{3+} + SO_4^{2-} + Cu$	$E_{total}^{\ 0} = -0.425V$

As highlighted in green, the water oxidation anode reaction requires a considerably higher energy input (1.229V) than does the Fe(II)/Fe(III) reaction (0.770V), while the cathode reactions are identical for the conventional and AART processes. Based on thermodynamics, AART reduces the overall voltage input for electrode reactions by over 50% (from 0.884 to 0.425V). Also, because there is no gas generation in the AART anode reaction, acid misting is completely eliminated. These results have been demonstrated and documented in several different studies, each of which noted the importance of using dimensionally stable anodes (DSA's) to achieve the highest reduction in required cell voltage (Sandoval and Lei, 1993), (Sandoval et al., 1995) and (Sandoval and Dolinar, 1996). DSA's promote uniform current density and, consequently, uniform cathode plating.

It should be noted that total power consumption for EW includes both that associated with the cell voltage and pumping power. In conventional EW, O_2 generation provides some electrolyte mixing, which is important for maintaining ion concentrations around the electrodes for reaction. Since mixing caused by O_2 is absent in AART pumping power must be increased to compensate. In a 1995 study by Sandoval and Dolinar, this aspect was examined specifically and results showed that at optimal cell injection configuration the total power associated with AART was roughly 60% of conventional EW. Even considering additional operations (e.g., Fe(II) regeneration and acid recovery), presumably, the total cost of commercial copper production using AART will be substantially lower than using conventional EW, however published cost data is currently unavailable.

A key factor for utilizing AART is the regeneration of Fe(II), as mentioned above, because electrolyte iron concentrations must be maintained for a balanced process. The proposed method of regeneration is by reduction of the Fe(III) produced at the anode by SO_2; the Fe(II)/ Fe(III) anode reaction combined with the Fe(II) regeneration using SO_2 is abbreviated FFS. This process should occur during electrolyte recycling as shown in the generalized schematic in Figure 1.1.

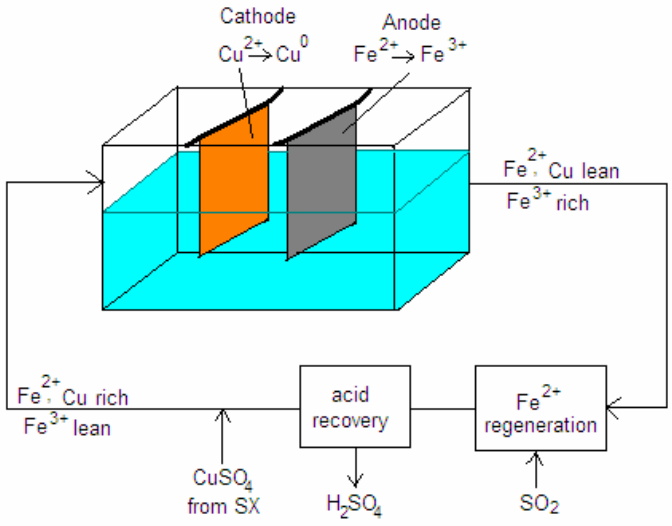

Figure 1.1 – General AART Process Using FFS

An additional benefit of AART using FFS is recoverable H_2SO_4, a byproduct of the Fe(II) regeneration that may be used in subsequent leaching operations. The Fe(II) regeneration reaction is written as shown in Equation 1,

$$SO_2 + 2Fe^{3+} + 2H_2O \rightarrow 2Fe^{2+} + SO_4^{2-} + 4H^+ \quad (1)$$

whereby, when considering an overall reaction with the copper sulfate ($CuSO_4$) in the electrolyte, two moles of H_2SO_4 are formed for every mole of metallic copper (Cu) plated; this is twice the amount of acid needed to maintain the electrolyte concentration, so one mole should be extracted to balance the system. Different schemes have been proposed for acid recovery, including an SX extraction demonstrated by Sandoval et al. in 1990.

The major benefits of AART using FFS as compared to conventional EW can be summarized as follows:

- substantial power reduction and, hence, cost savings and environmental benefits for copper hydrometallurgy;
- elimination of acid misting and associated problems;
- by-production of recoverable acid, which might be used for leaching operations.

As further indication for the potential success of this technology, a pilot study has been undertaken by Phelps Dodge with positive results, though specifics are protected by confidentiality agreements.

While AART using FFS appears promising, several areas necessitate further research before commercialization is likely. Such areas include optimization of acid recovery methods, anode types, and the Fe(II) regeneration process. This process has several variables and is complicated by the fact that the reduction of Fe(III) by SO_2 is known to be naturally slow, thus requiring a catalyst (Sandoval and Dolinar, 1996). Further description of the process, the importance of understanding and optimizing the system, and two studies, one from an industrial and the other from a more fundamental perspective, follow.

Ferrous Iron Regeneration Using Sulfur Dioxide

Fe(II) regeneration is critical to AART using FFS in order to achieve a balanced system with sufficiently constant concentrations of Fe(II) and Fe(III); there must be adequate Fe(II) supplied to EW cells for the anode reaction, and the Fe(II)/Fe(III) ratio must be maintained to control cell voltage.

The Reaction

As stated above, the method of Fe(II) regeneration for AART using FFS uses SO_2 to reduce the Fe(III) generated by the EW anode reaction. Based on stoichiometry, one mole of SO_2 can reduce two moles of Fe(III) to Fe(II) via a two-electron transfer as shown in the addition of the two half reactions below in Equation 2:

$$\begin{array}{rl} & SO_2 + 2H_2O \rightarrow 2e^- + SO_4^{2-} + 4H^+ \\ + & 2Fe^{3+} + 2e^- \rightarrow 2Fe^{2+} \\ \hline & SO_2 + 2Fe^{3+} + 2H_2O \rightarrow 2Fe^{2+} + SO_4^{2-} + 4H^+ \end{array} \qquad (2)$$

Equilibria are very complex for sulfur oxides and constitute an entire field of study for inorganic chemists, but the following is the general solution chemistry for dissolved SO_2. For the AART using FFS process, SO_2 is introduced as a gas into the (airtight) Fe(III)-rich electrolyte, upon which it dissolves into the solution as aqueous SO_2 and [theoretically] forms sulfurous acid (H_2SO_3), an anhydrous oxide. H_2SO_3 is very unstable; in fact, it cannot be detected spectroscopically in solution, and de-protonates and dissociates immediately (Shriver and Atkins, 2003). The degree to which the first de-protonation to bisulfite (HSO_3^-) occurs is much greater than that of the second de-protonation to sulfite (SO_3^{2-}), as dictated by their respective equilibrium constants. The following (Equations 3-6) represents the behavior of SO_2 in aqueous solution as is applicable to FFS:

$$SO_{2(g)} \Leftrightarrow SO_{2(aq)} \qquad (3)$$

$$SO_{2(aq)} + H_2 0 \Leftrightarrow H_2SO_3 \qquad (4)$$

$$H_2SO_3 \Leftrightarrow HSO_3^- + H^+ .....K = 1.4\times10^{-2} \qquad (5)$$

$$HSO_3^- \Leftrightarrow SO_3^{2-} + H^+ .....K = 6.3\times10^{-8} \qquad (6)$$

Since H_2SO_3 is known to be so unstable and undetectable in solution, it is assumed that it dissociates completely to $SO_{2(aq)}$ and water, such that the acid really only exists as a way of explaining the formation of HSO_3^- and SO_3^{2-} with common concepts in acid chemistry. Upon $SO_{2(g)}$ dissolving into the electrolyte, the potential sulfur containing species in solution are then $SO_{2(aq)}$, HSO_3^- and SO_3^{2-}; given the equilibrium constants, the amount of SO_3^{2-} is very small as compared to the other species, and given the high acidity of electrolyte, $SO_{2(aq)}$ will be far more prevalent than HSO_3^-, as is discussed below. The above suppositions are supported by several studies of aqueous phase SO_2 oxidation (Kumar et al., 1996) and (Govindarao and Gopalakrishna, 1995).

The sulfur species are met by Fe(III) ions in the electrolyte solution and subsequently react, reducing the Fe(III) and oxidizing the S(IV). Since the homogeneous reaction occurs slowly, the reaction must be catalyzed in practice by passing the electrolyte containing the reactants through a bed of activated carbon. Also worth considering is the possibility that Fe(II) ions might react with dissolved O_2 in the solution and be oxidized, opposing the desired increase in Fe(II) concentration; however, this does not seem likely during Fe(II) regeneration since the reactor should be airtight.

Important to note are the conditions under which Fe(II) regeneration must occur, most of which are dictated by the typical nature of EW electrolyte solutions:

- high temperature,
- high molar acidity,
- specific Fe(III):Fe(II) ratios,
- and high flow rate.

Literature Review

While Fe(II) regeneration by SO_2 has been successfully managed in both bench and pilot scale testing of AART using FFS, there is little published about the regeneration reaction itself, as testing has tended to focus on issues surrounding EW (i.e., cell voltage, pumping power, current density). Few studies outside of the realm of AART are found that

examined the reaction specifically, although one in particular had some significant similarities despite being conducted under differing conditions and with differing goals. Additionally, several articles were found in the literature that examined similar reactions (e.g., Fe(III) reduction, separately, SO_2 oxidation, catalyzed by carbon or a comparable catalyst), however, none at anywhere near the extreme conditions encountered in EW electrolytes (e.g., high acidity and temperature).

Sandoval and Lei reported in 1993 that the Fe(III) reduction by SO_2 could be accelerated by increasing temperature and also that increasing total iron concentration negatively affected the reaction. The reaction was later observed by Sandoval and Dolinar to be catalyzed by passing the reactants (contained in electrolyte) through a bed of activated carbon, although little information was reported on specific reaction mechanisms or kinetics. Other similar reduction-oxidation reactions are also known to be catalyzed this way, notably, one of the relevant half-reactions in Fe(II) regeneration, the reduction of Fe(III) to Fe(II). Thomas and Ingraham studied this reaction using oxygen as a reducer, and tested both $CuSO_4$ and activated carbon as catalysts. The reaction rate was reported to have increased 14-fold and 2400-fold, respectively, in the presence of the listed catalysts.

The Thomas and Ingraham study perceived the general mechanism of catalysis to be the provision of surface area onto which the reactants could adsorb, thereby allowing the reaction to occur. As such, the effect of surface area was examined as part of the study and, as expected, increased surface area greatly increased the rate of reaction. (Further explanation regarding the mechanism of catalysis by materials such as activated carbon is addressed below.) Other variables determined to be of importance to the reaction rate were temperature, acidity, and concentrations of reactants and products, which seem likely as influences on the Fe(II) regeneration process also. The study also concluded that the activity of the carbon catalyst could be retained for relatively long periods of time.

With respect to the other relevant half-reaction, SO_2 oxidation, there are also published studies in which the surface of a solid was utilized as a catalyst; differing reaction limitations were reported. Seaburn and Engel concluded in a 1973 study that the rate of

aqueous SO_2 oxidation by dissolved O_2 was controlled by adsorption of $SO_{2(aq)}$ onto the catalyst, activated carbon. With respect to the oxidized species, this conclusion is disputed in a more recent study also using activated carbon as a catalyst for the reaction. Of the detected S(IV) species, HSO_3^- and $SO_{2(aq)}$, it was reported that HSO_3^- was the oxidized species and $SO_{2(aq)}$ was non-reactive (Govindarao and Gopalakrishna, 1995). Furthermore, it was observed that the $SO_{2(aq)}$ had a deactivating effect on the catalyst due to its competition with HSO_3^- for adsorption sites and its retention on the catalyst surface after adsorption. This blinding effect was also observed in a similar study using poly-4-vinylpyridine-Cu as a catalyst (Kumar et al., 1996).

Yet another study of aqueous SO_2 oxidation by O_2, again in the presence of activated carbon, examined reaction kinetics and found that the reaction was limited by solution acidity, which limited aqueous oxidant concentration since with increased acid concentration, O_2 becomes less soluble (Komiyama and Smith, 1975).

The specific limitations and catalyst blinding experienced in the previous SO_2 oxidation studies are not expected to be problematic in the Fe(II) regeneration, although similar phenomena could occur. First, as mentioned above, at high acid concentrations – pH below two – $SO_{2(aq)}$, not HSO_3^-, is the predominant species when $SO_{2(g)}$ is dissolved (Govindarao and Gopalakrishna, 1995), (Garcia et al., 1998) and (Krissman et al., 1998). Since typical electrolyte pH encountered in Fe(II) regeneration is well below two, $SO_{2(aq)}$ will be the species oxidized. $SO_{2(aq)}$ is not easily oxidized by O_2, but it is by Fe(III). Next, while the oxidant, Fe(III), is fully soluble in the acidity and temperature ranges typical for EW electrolytes, the reducer, S(IV), may be difficult to keep dissolved, due to its partial pressure, if reactors are not kept airtight. Finally, any catalyst deactivation by non-reactive species would have to be caused by Fe(II) adsorption, which will be non-reactive in the absence of O_2; however, since published diffusivity data indicates that $SO_{2(aq)}$ reaches the catalyst surface much faster than iron ions, deactivation is not expected to occur (Han, 1990), (Freiberg and Schwartz, 1981) and (Ramsing and Gundersen, no year given).

To further increase the reaction rate of aqueous SO_2 oxidation by O_2, electro-catalysts have been investigated, including the use of transition metals as mediators to provide an alternate reaction route between the catalyst and reacting species (Garcia et al., 1998) (Berglund et al, 1993). The Fe(II)/Fe(III) reduction-oxidation couple has been the subject of experimentation for this purpose, and so associated literature may be reversibly applicable to the Fe(II) regeneration process, accounting for both relevant half-reactions (Fe(III) reduction and SO_2 oxidation).

A particular study conducted by Garcia et al. in 1998 examined aqueous SO_2 oxidation with an Fe(II)/Fe(III) iron cycle in the presence of dissolved O_2 and graphite, a catalyst similar to activated carbon but of much lower surface area, whereby Fe(III) was generated by Fe(II) oxidation and then used to oxidize the SO_2. It should be noted that while the above study bears some similarities to the process of current interest, it was conducted under different conditions (i.e., slightly lower molar acidity, lower temperature, differing Fe(III), Fe(II), SO_2 ratios, and batch-type tests rather than continuous flow) than the Fe(II) regeneration must be and with different goals in mind.

At 3M H_2SO_4, all of the S(IV) was assumed to be of the form $SO_{2(aq)}$ – as will be the case in Fe(II) regeneration – which behaved differently in the absence and presence of Fe(III). With only Fe(II) and $SO_{2(aq)}$ in solution with dissolved O_2, the $SO_{2(aq)}$ was almost non-reactive and the Fe(II) oxidation occurred rapidly. This result is in agreement with other studies on aqueous S(IV) oxidation, which concluded that the $SO_{2(aq)}$ species was not oxidized by O_2, but that HSO_3^- was. For the Fe(II) regeneration process, the absence of $SO_{2(aq)}$ oxidation gives some insight into consequences of disproportional ratios of Fe(III) to SO_2 ratios: if ample Fe(III) is not available for reaction, $SO_{2(aq)}$ may not be reacted, producing problems in the EW electrolyte circuit (e.g., $SO_{2(g)}$ escape or depleted acid concentration). Also, if any O_2 is present in the electrolyte, Fe(II) will rapidly oxidize and counteract the desired process results.

As for $SO_{2(aq)}$ behavior when Fe(III) was introduced, in batch tests of solutions containing $SO_{2(aq)}$, Fe(II) and Fe(III) with dissolved O_2, $SO_{2(aq)}$ was readily oxidized.

Additionally, it was observed that the oxidation was inhibited somewhat by Fe(II), due in part to both the initial Fe(II) concentration and that produced by Fe(III) reduction. This inhibition, which was explained by the competitive adsorption of Fe(II) on the catalyst, will be to a lesser extent for the Fe(II) regeneration process, if present at all. The regeneration process is continuous flow and the activated carbon catalyst should provide a larger number of surface sites for adsorption, as opposed to the graphite used in the above study.

Although catalysts like carbon may provide two mechanisms of catalysis for reduction-oxidation reactions, surface adsorption and electron transfer, this was not found to be the case for the Fe(III)-$SO_{2(aq)}$ reaction in the above study. Instead, it was proposed that under the conditions studied, iron ions adsorbed onto the catalyst surface, inhibiting adsorption of $SO_{2(aq)}$ molecules, and surface-bound Fe(III) reacted with $SO_{2(aq)}$ in solution, meaning the reaction was only catalyzed by adsorption of one species, and not by electron transfer through the solid. However, that mechanism does not seem plausible for the Fe(II) regeneration process considering published diffusion coefficients. It is more probable that the $SO_{2(aq)}$ will quickly adsorb onto the carbon surface, followed by iron ions; Fe(III) will immediately react with the $SO_{2(aq)}$ and Fe(II) will be non-reactive so long as dissolved O_2 is negligible.

Regarding other major findings during review of the pertinent literature, one similarity between studies involving SO_2 was the problematic nature of SO_2 measurement. Iodimetry was used to directly measure SO_2 in solution; although several authors noted issues with loss of concentration during sample measurement and/or transport, and also with separation if multiple species were present that might react with the triiodide used during titration (Kumar et al., 1996), (Govindarao and Gopalakrishna, 1995) and (Garcia et al., 1998). As well, several attempts were made in the current work to convert aqueous SO_2 to gaseous phase for measurement. This method proved difficult and inaccurate due to the complexity of procedures required to drive all SO_2 out of solution and capture it within a known volume. In the 1998 Garcia et al. study, indirect measurements - determining changes in SO_2 concentration by stoichiometry with other measurable quantities – were reported to be more accurate than direct methods. An SO_2-specific probe was found to be available during

a literature search on aqueous SO_2 measurement; however, the probe was observed to be unreliable during tests (Cook, 2004).

The Fe(II) regeneration process in AART using FFS is certainly complex and various issues must be considered to study it. Combining general knowledge about solution and catalysis chemistry with given process conditions and a review of reactions similar to those of interest, several major points become clear:

- There are a number of variables that might affect the process, which may or may not be dependent on each other;
- The kinetics of the process are likely governed by the rate of surface adsorption of reactant(s) onto the catalyst;
- Measurement of SO_2 concentrations may prove problematic.

Objectives

A better understanding of the Fe(II) regeneration process may prove beneficial in numerous areas, including design and improvement of the process, its place within the EW circuit, equipment and materials. Lessons learned with respect to the Fe(II) regeneration might also shed light on other similar processes. With the above points in mind, it is possible to study the regeneration from at least two perspectives, the first being a fundamental look at the regeneration reaction and the second an industrial type optimization. For optimization, it may only be necessary to relate the process outputs to the inputs, and then determine the combination of input variables producing the most desirable results. This type of study is quite common industrially, and can provide information for both improving a current process and designing a new process or operation. For a fundamental study, it is still important to relate process outputs to inputs, however a closer look might also be taken at the mechanics of the relationship. With respect to the Fe(II) regeneration, process factors might be related to results by the chemical reaction mechanisms occurring within the process. Through an internal understanding of a process, a more fundamental perspective can also provide insight into potential improvements.

Scope

To examine what factors affect the Fe(II) regeneration process, and how and why they affect it, the two studies below were designed and conducted, and the details are contained in the following papers. The studies were completed concurrently, so the design of one was not typically dependent on the other.

Fundamental Kinetics

For a better internal understanding of the Fe(II) regeneration process, a model of the fundamental kinetics was developed. The goal of the modeling process was to capture the major reaction mechanism(s) and quantify the specific rate constant(s). General knowledge was combined with observations of comparable reviewed reactions and a basic kinetic model was hypothesized for the Fe(II) regeneration. Based on the model, variable process factors expected to be most influential to the reaction rate were carbon surface area, initial Fe(III) concentration and flow rate. The model was validated experimentally by collecting data relating process variables to the reaction rate. The final model provides insight into both the current process and other processes with analogous reaction mechanisms.

Empirical Optimization

For the purpose of improving the current Fe(II) regeneration process, an empirical optimization was completed. The goal was to maximize throughput at an acceptable level of Fe(III) reduction (Fe(II) regeneration) and without "breakthrough" (un-reacted) SO_2 in the effluent, which is potentially hazardous. Again, general knowledge and the literature defined influential factors, which were varied over operable ranges during experimentation, to examine their effects on process responses. Factors considered most important and included in the optimization were carbon surface area, initial Fe(III) and SO_2 concentrations, and temperature. Design Expert, a software package by Stat-Ease, was utilized in experimental design, to analyze and model experimental data, and, then, to optimize the process. Both the model and optimization results may be useful in Fe(II) regeneration process design and improvement.

Chapter 2: Fundamental Kinetics of the Ferrous Regeneration for Alternate Anode Reaction Technology

Emily Allyn Sarver

Abstract

The Fe(II) regeneration process is an important aspect of Alternate Anode Reaction Technology (AART) using a Fe(II)/Fe(III)-SO_2 (FFS) for copper hydrometallurgy. The process is basically Fe(III) reduction by $SO_{2(aq)}$, which is catalyzed by activated carbon particles. For the current work, experiments have been conducted to examine the fundamental kinetics of the process, including the primary reaction mechanism and the effects of four variable factors – carbon particle size, flow rate, and initial Fe(III) and SO_2 concentrations – on the Fe(II) regeneration rate. As expected, the regeneration reaction is mass transfer-controlled, and the rate is limited by the diffusivity of Fe(III). Carbon particle size and initial Fe(III) are the most influential factors under the conditions tested. Additionally, initial SO_2 concentration has been determined to be insignificant to the reaction rate, and flow rate affects the reaction rate via its affects on diffusivity. The following rate expression has been hypothesized and validated by experimental data, with the diffusivity of the Fe(III) ions being observed as 1.1×10^{-7} cm^2/s.

$$\frac{dFe^{2+}}{dt} = \frac{6M}{\rho d V}\left[\frac{2D_f}{d} + 0.6\frac{V_t^{1/2} D_f^{2/3}}{d^{1/2} \nu^{1/6}}\right][C_{Fe^{3+}}]$$

Introduction

Copper is currently the third most used metal in the world, primarily because of its exceptional electrical conductivity and resistance to corrosion. In 2003, about 17 million metric tons of copper were produced to supply the growing global demand (ICGS, 2003). In addition to increasing demand, copper prices have also been on the rise, skyrocketing to over $1.50 per pound in April 2005, up from just $0.68 only two years earlier (LME, 2005). Rising prices are due in part to growing production costs, which are not expected to decline to previous levels when energy was less expensive. High prices present a real advantage to low-cost producers, and new technologies that are capable of cutting costs are under serious consideration by the copper industry. One such technology – alternate anode reaction technology (AART) – has shown potential for a major reduction in power consumption, a primary cost center for electrowinning (EW) in hydrometallurgical production of copper (Sandoval and Lei, 1993; Sandoval et al., 1995; Sandoval and Dolinar, 1996).

AART basically changes the conventional EW anode reaction from water oxidation to ferrous (Fe(II)) to ferric (Fe(III)) iron oxidation, while the cathode reaction remains the same. This change results in two major advantages over the conventional process: substantial reduction in overall energy (power) requirements for EW and elimination of hazardous acid misting. The power reduction can be attributed to the reduced equilibrium potential of the alternate anode reaction, and the elimination of acid misting to the absence of O_2 production at the anode, which is present with the conventional anode reaction. One major aspect of the above AART is the necessity of Fe(II) regeneration – reducing the Fe(III) produced at the anode back to Fe(II) – to maintain recyclable EW electrolyte streams.

The method of regeneration that has been most successful during testing is Fe(III) reduction by SO_2. This method is attractive because SO_2 can be potentially obtained from nearby copper smelters, relatively easily and inexpensively. Also, the use of SO_2 as the reducer produces recoverable sulfuric acid as a by-product, which is beneficial because the acid may be utilized in leaching operations or sold (Sandoval and Dolinar, 1996). The

combination of the Fe(II)-Fe(III) anode reaction and the subsequent Fe(II) regeneration by SO_2 is abbreviated FFS. The FFS electrode reactions for copper EW and the Fe(II) regeneration reaction are shown below in Equations 1-4.

Anode reaction: $2\times(Fe^{2+} \rightarrow Fe^{3+} + e^{-})$ (1)

Cathode reaction: $CuSO_4 + 2e^{-} \rightarrow Cu^{0} + SO_4^{2-}$ (2)

Overall EW reaction: $CuSO_4 + 2Fe^{2+} \rightarrow Cu^{0} + SO_4^{2-} + 2Fe^{3+}$ (3)

Fe(II) regeneration reaction: $SO_2 + 2Fe^{3+} + 2H_2O \rightarrow 2Fe^{2+} + SO_4^{2-} + 4H^{+}$ (4)

As can be seen above, for every mole of plated copper (Cu^0), two moles of Fe(III) are generated at the anode and must be reduced back to Fe(II) by a mole of SO_2. In practice, the SO_2 is injected into the Fe(III)-rich electrolyte after it leaves the EW cells, and then the solution is passed through a bed of activated carbon where the regeneration reaction occurs, shown in Figure 2.1. The role of the activated carbon is as a catalyst, which is discussed below. The recoverable acid by-product is produced when the excess H^+ in Equation 4 reacts with the copper sulfate ($CuSO_4$) already contained in the electrolyte.

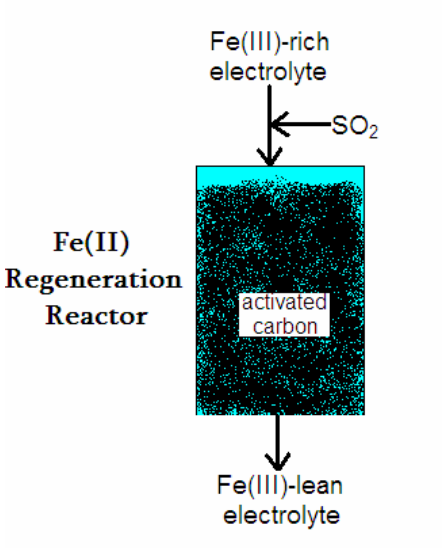

Figure 2.1 – Fe(II) Regeneration Reactor for AART Using FFS

Although the Fe(II) regeneration process has been successfully managed during both bench and pilot scale testing of AART using FFS, little has been done to study it specifically. A basic understanding of the reaction mechanism(s) and kinetics surrounding the

regeneration may provide insight into the current process or other similar processes. Such understanding may be helpful in design or optimization of a process, a circuit, or equipment, and potentially improve process results or efficiency or save costs. As such, the objective of the current work was to develop a fundamental rate model for the Fe(II) regeneration. To do so, it was first necessary to determine factors potentially affecting the regeneration and the most probable reaction mechanism, such that a model could be hypothesized. Experimental data were then collected and used to fit unknown model terms.

Fundamental Rate Model Development

Following is the development of a fundamental rate model for the Fe(II) regeneration process, supported by a review of relevant literature and principles of reaction mechanics and kinetics.

First, the regeneration reaction given in Equation 4 accounts for the overall reaction, whereby the end products of the reaction between SO_2 and Fe(III) in aqueous solution are S(VI) (as sulfuric acid) and Fe(II); however, Equation 4 does not address any intermediate reactions, the specific S(IV) species oxidized or the implications of such details. For the Fe(II) regeneration, SO_2 is introduced as a gas into the electrolyte before it enters the reactor. A review of SO_2 solution chemistry provides the following series of reactions (Equations 5-8) that may occur upon dissolution of gaseous SO_2 in aqueous solution:

$$SO_{2(g)} \Leftrightarrow SO_{2(aq)} \quad (5)$$

$$SO_{2(aq)} + H_2 0 \Leftrightarrow H_2SO_3 \quad (6)$$

$$H_2SO_3 \Leftrightarrow HSO_3^- + H^+ .....K = 1.4\times10^{-2} \quad (7)$$

$$HSO_3^- \Leftrightarrow SO_3^{2-} + H^+ .....K = 6.3\times10^{-8} \quad (8)$$

When dissolved, SO_2 may be of the form $SO_{2(aq)}$, or form sulfurous acid (H_2SO_3) and immediately dissociate to bisulfite (HSO_3^-) or sulfite (SO_3^{2-}) as shown above. H_2SO_3 is so unstable that it is virtually undetectable spectroscopically in solution and will, therefore, not be significant in the Fe(II) regeneration (Shriver and Atkins, 2003). Also, due to the relative dissociation constants in Equations 7 and 8, SO_3^{2-} concentration will also be negligible or nonexistent, leaving $SO_{2(aq)}$ and HSO_3^- as possible species. The acidity of the electrolyte will

play a major role in determining the extent of each. It has been established that in highly acidic solutions– below pH of about 2 – $SO_{2(aq)}$ is the predominant species upon dissolution of $SO_{2(g)}$ (Krissman et al., 1998; Govindarao and Gopalakrishna, 1995). Due to the extreme acid concentration – nearly 4M – of the electrolyte in the Fe(II) regeneration process, it can be safely assumed that essentially all of the dissolved SO_2 will be of the form $SO_{2(aq)}$. As such, intermediate reactions were not considered in the rate model development.

Unfortunately, it has also been observed that the homogeneous reaction between S(IV) and Fe(III) is much slower when $SO_{2(aq)}$ is the reacting species rather than HSO_3^- (Garcia, et al., 1998). Specifically under the conditions encountered in the Fe(II) regeneration, the slowness of the Fe(III)-$SO_{2(aq)}$ reaction was reported separately by Sandoval and Dolinar in 1996. While the reaction rate can be increased by catalysis as discussed below, electrolyte acid concentration cannot be changed without significantly affecting other operations within the scheme of EW, and the entire hydrometallurgical process including leaching and solvent extraction. Therefore, the rate model developed in the current work is specific to a Fe(III)-$SO_{2(aq)}$ reaction in solutions of high acidity.

For the Fe(II) regeneration, the reaction rate can first be expressed generically and then expanded to include the mechanism(s) and/or known process factors, like flow rate. Rate expressions for chemical processes are typically written as a function of the reactants and products of the process – irreversible processes only require known concentrations of either reactants or products. The Fe(II) regeneration reaction (Equation 4) may be assumed irreversible, and if the reactants, Fe(III) and $SO_{2(aq)}$, react only with each other (i.e., the consumption ratio of each reactant is dictated by the reaction stoichiometry), a rate expression of the simplest form may be applied. Such an expression is shown in Equation 9, whereby the rate of depletion of Fe(III), $-\frac{dFe^{3+}}{dt}$, is related to the initial concentrations of both reactants, $C_{Fe^{3+}}$ and C_{SO_2}, by a rate constant, k.

$$-\frac{dFe^{3+}}{dt} = k[C_{Fe^{3+}}]^x[C_{SO_2}]^y \qquad (9)$$

The orders of the reaction, x and y, represent the relative influence of each reactant, Fe(III) and $SO_{2(aq)}$, respectively. Since the amount of Fe(III) consumed in the reaction is equal to the amount of Fe(II) produced, the rate of the regeneration can be expressed as follows in Equation 10.

$$\frac{dFe^{2+}}{dt} = k[C_{Fe^{3+}}]^x[C_{SO_2}]^y \qquad (10)$$

As written, k accounts for the two to one, Fe(III)-SO_2 consumption ratio (i.e., for an equation to express the rate of change in $SO_{2(aq)}$, the rate constant would be one-half of the value of k). It also encompasses all process factors other than the initial reactant concentrations and the reaction time, dt. For the Fe(II) regeneration, dt is the incremental time in which the concentration of Fe(II) changes. In this continuous flowing system, dt is also assumed to be the same as the retention time of the solution in the column of activated carbon. The retention time, τ, can be easily determined if the electrolyte volume, V, and flow rate, F, through the carbon are known, Equation 11.

$$\tau = \frac{V}{F} \qquad (11)$$

If the concentration of one reactant can be held constant during the reaction, the rate limiting reactant and reaction order can be established. It was not possible to do this experimentally in the case of SO_2 because high residual SO_2 concentration would have impacted analysis of Fe(II). However, it may be assumed that the reaction is controlled by the diffusion of Fe(III) through the boundary layer, since the diffusivity of Fe(III) is 3.5×10^{-6} cm^2/s (Han, 1990) and that of $SO_{2(aq)}$ is 3.0×10^{-5} cm^2/s (Ramsing and Gundersen, no date given). As such, the order of SO_2 should be much lower than that of Fe(III) (i.e., $x >> y$) and Equation 10 can be re-written as Equation 12:

$$\frac{dFe^{2+}}{dt} = k'[C_{Fe^{3+}}]^x \qquad (12)$$

For mass transfer-controlled reactions, $x = 1$. Also, since the concentration of $SO_{2(aq)}$ should not influence the reaction rate, $[C_{SO_2}]^y$ can now be included in the apparent rate constant, k'. To further define k', a more in depth understanding of the Fe(II) regeneration reaction is required, particularly with respect to the reaction mechanism.

As stated above, since the homogeneous reaction between Fe(III) and $SO_{2(aq)}$ has been observed to be very slow, catalysts are needed for this reaction, and activated carbon has been successfully utilized (Sandoval and Dolinar, 1996; Sandoval et al, 1995). The carbon provides a surface on which the reaction can occur, and its success as a catalyst, like that of other similar materials, has been well documented for reduction-oxidation reactions. In fact, surface catalysts have been shown to increase reaction rates by up to three orders of magnitude for both SO_2 oxidation and Fe(III) reduction in aqueous solution (Thomas and Ingraham, 1963; Komiyama and Smith,1975; Govindarao and Gopalakrishna, 1995). The primary mechanism of catalysis is generally supposed to be the provision of adsorption sites for reactants, although electron transfer through the solid catalyst is also proposed as a secondary mechanism for reduction-oxidation reactions (Garcia et al., 1998). Since adsorption is highly dependent on surface area, that of the activated carbon was presumed to be of major importance to the regeneration rate model. Additionally, because the rate of the reaction has been observed to be so much faster than that of the homogeneous reaction (Sandoval and Dolinar, 1996), the Fe(II) regeneration rate model was developed for a purely mass transfer-controlled reaction, meaning that the products of collision-controlled reactions in solution were assumed negligible. Evidence supporting this assumption is also found in a study by Garcia et al. (1998), where the extent of the homogeneous reaction between Fe(III) and SO_2 in the presence of a surface catalyst proved insignificant.

For purely mass transfer-controlled Fe(II) regeneration, complete reaction requires that one $SO_{2(aq)}$ ion and two Fe(III) ions must adsorb on the carbon surface as depicted in Figure 2.2.

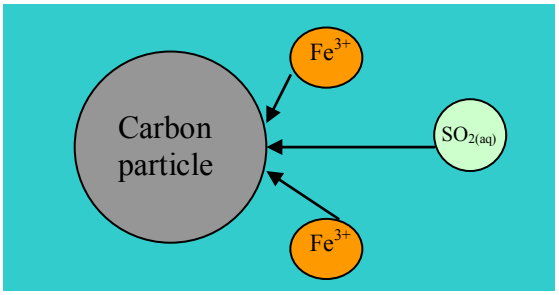

Figure 2.2 – Depiction of Fe(II) Regeneration Reaction Mechanism

The Fe(II) regeneration can be described as a particulate system of carbon particles within an electrolyte matrix. The rate constant, k_m, for a mass transfer reaction in a particulate system is of the form of Equation 13 (Han, 2002).

$$k_m = \frac{2D_f}{d} + 0.6\frac{V_t^{1/2} D_f^{2/3}}{d^{1/2} v^{1/6}} \tag{13}$$

D_f is the diffusion coefficient of an adsorbing species, d is the mean diameter of carbon particles, v is the kinematic viscosity of the electrolyte solution, and V_t is slip velocity, which for the Fe(II) regeneration system is given by Equation 14.

$$V_t = \frac{F}{A_s} \tag{14}$$

Slip velocity represents the difference in flow rates of materials or fluids; for the Fe(II) regeneration system, since the carbon particles are stationary, V_t gives the flow of the electrolyte around them. A_s is then the cross-sectional area of the reactor through which electrolyte solution can flow (i.e., the area not occupied by the carbon particles). Additionally, v can be calculated by Equation 15 as the quotient of the dynamic viscosity of water at the reaction temperature, μ_w, and the density of the electrolyte, ρ_s.

$$v = \frac{\mu_w}{\rho_s} \tag{15}$$

D_f is expressed in units of area per time, representing the rate at which a species can diffuse through a boundary layer. For the Fe(II) regeneration, this quantity can be understood as the rate at which a species diffuses and adsorbs onto the carbon surface. Since, per the above developments adsorption of all reactants is required prior to reaction, the rate limiting reactant will be the one with the slower adsorption rate (i.e., lower D_f value.). Factors known to influence diffusivity include temperature, size of the diffusing species, molar concentration, and acidity of the solute (Han, 1990). Diffusivities of the reactants for the current work are expected to be somewhat different from the published values due to differing process conditions, including acidity, temperature and the continuous flow nature of the current experiments, as opposed to the batch tests from which the above diffusivity data

were determined. However, there is still expected to be a large degree of separation between the Fe(III) and $SO_{2(aq)}$ diffusion coefficients, since both reactants will be subject to the same process conditions during the Fe(II) regeneration and should, consequently, experience the same types of changes in diffusivity. As such, Equation 12, which assumes that Fe(III) is the rate limiting reactant, is expected to be valid for the regeneration. Analysis was conducted for verification as shown in the Results and Discussion section below.

In order to adapt the general rate expression of Equation 12 to apply to the mass transfer-controlled Fe(II) regeneration, both k_m and a term representing the potential contact between the reactants and the carbon surface must be incorporated into *k'*. The contact can be expressed in terms of the fixed volume of electrolyte (containing the reactants), *V*, around the surface area of carbon particles, *A*, in the reactor. The rate expression then becomes Equation 16, where the order of reaction, *x*, is excluded since it should be equal to one for the mass transfer reaction.

$$\frac{dFe^{2+}}{dt} = \frac{A}{V}\left[\frac{2D_f}{d} + 0.6\frac{V_t^{1/2}D_f^{2/3}}{d^{1/2}\nu^{1/6}}\right][C_{Fe^{3+}}] \qquad (16)$$

Finally, if the carbon particles are assumed to be spheres, *A* can be expressed in terms of the carbon mass, *M*, density, ρ, and mean diameter, *d*, and Equation 16 becomes Equation 17, the final hypothesized rate model.

$$\frac{dFe^{2+}}{dt} = \frac{6M}{\rho dV}\left[\frac{2D_f}{d} + 0.6\frac{V_t^{1/2}D_f^{2/3}}{d^{1/2}\nu^{1/6}}\right][C_{Fe^{3+}}] \qquad (17)$$

By examining Equation 17, the factors likely to influence the Fe(II) regeneration were identified. First, carbon particle size was expected to have a large effect on the reaction rate as was mentioned previously. If the particle size is reduced, the reaction rate should increase significantly. It should also be noted that carbon density varies slightly with particle size (due to the decrease in porosity with decreasing size), so this had to be considered when fitting the model to experimental data. Flow rate through the fixed volume reactor will affect Fe(II) regeneration in two ways: by dictating the retention time and the slip velocity term.

Since the reaction is expected to be first-order, which should be verified experimentally, the only unknown quantity is the Fe(III) diffusion coefficient.

Acidity of the Fe(II) regeneration cannot be changed for the reasons stated previously, which also apply to the solute concentrations, since various other copper hydrometallurgical operations require specific concentrations. Regarding temperature, increased temperature positively affects reaction rates via a number of phenomena, most commonly through the provision of activation energy, or reduction of a thermal reaction boundary. However, separate experiments surrounding the Fe(II) regeneration process (associated with the optimization problem in Chapter 3) yielded complex results with respect to the significance of reaction temperature on rate. These results and some potential explanations are discussed in Chapter 3. An optimal temperature for the reaction, 120 °F, was observed during these experiments. This temperature is common for electrolytes in the Fe(II) regeneration area of EW circuits. Given the complexity of the results associated with the separate experiments, the observed success at an optimal temperature and the time necessary to gather sufficient data to conclude temperature dependence of the Fe(II) regeneration, the rate model developed in the current work is for Fe(II) regeneration at 120 °F.

Experimental

To collect data capturing the effects of carbon particle size, flow rate and the initial concentrations of Fe(III) and $SO_{2(aq)}$ on rate of regeneration, a bench-scale Fe(II) regeneration reactor was constructed. The reactor was operated under conditions similar to a larger-scale process (e.g., temperature, acidity, Fe(II) to Fe(III) ratio). All test work was completed at the SX/EW Test Facility, operated by the Phelps Dodge Process Technology Center in Morenci, AZ.

Apparatus and Materials

The apparatus for Fe(II) regeneration experiments consisted of the following parts:

- 12” Plexiglas column from Waters Equipment (1.45” internal diameter) with top and bottom mesh-covered screw-caps fitted for electrolyte and effluent flows; when filled with activated carbon, the column functioned as the Fe(II) regeneration reactor
- 150 lb pressurized SO_2 tank with a digitally-set Porter Instruments mass flow controller rated for 0-150 mL/min flow
- 20 L electrolyte mix tank with variable speed mixer, and coil immersion heater with Cole Parmer Dyna-Sense controller
- Cole Parmer Masterflex automatic-dispensing electrolyte pump rated for 4-480 mL/min flow with digital controller
- Catch tank, tubing and fittings, valves and check valves, thermometer, stopwatch, 15 mL sample tubes with airtight caps

The apparatus is shown in Figure 2.3.

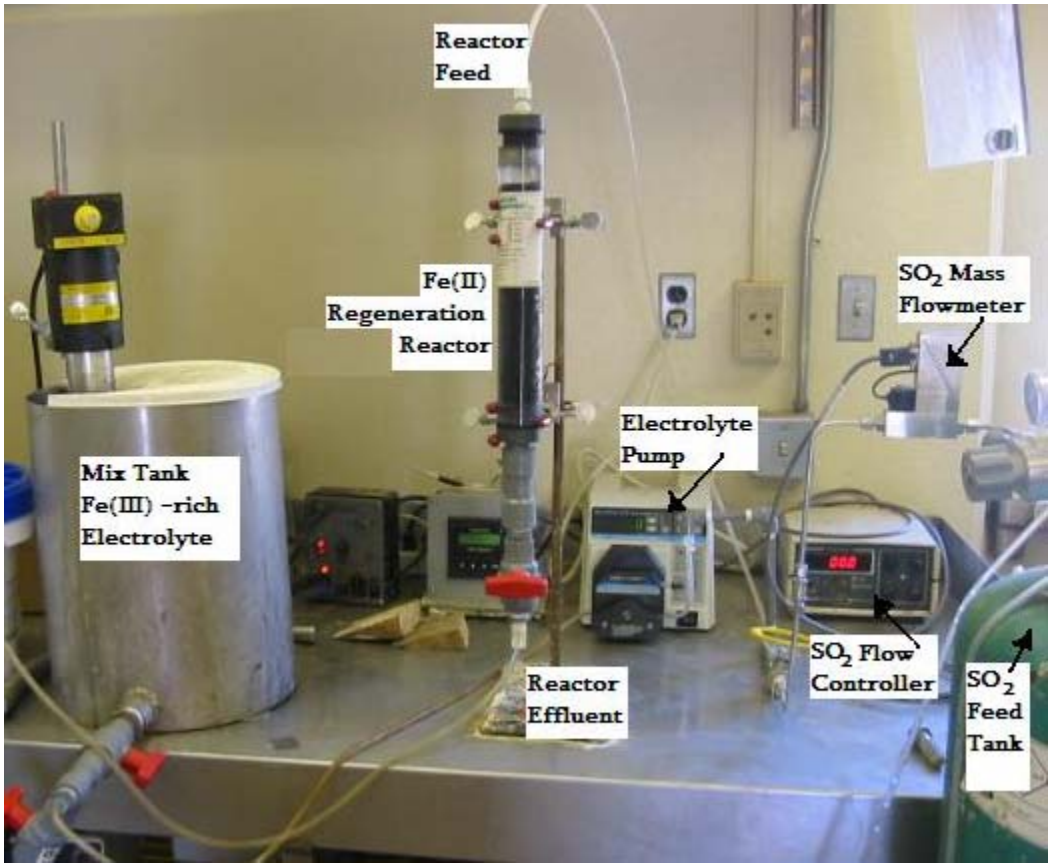

Figure 2.3 – Experimental Apparatus

Materials for the experiments consisted of the following:

- Electrolyte ingredients: reagent-grade sulfuric acid (97%), ferrous (100%) and ferric (76%) sulfates, technical-grade copper (II) sulfate (98%), and de-ionized water; reagent-grade chemicals were obtained from chemical the suppliers, Cole-Parmer and VWR, and the copper (II) sulfate was obtained from a Phelps Dodge refinery.
- Gaseous SO_2 (from pressurized tank)
- Activated carbon (of bituminous coal type) of three mesh class sizes: 12x40 (mean particle size 843 μm), 16x45 (mean particle size 649 μm) and 20x50 (mean particle size 499 μm); carbon was obtained from TIGG, but as 16x45 mesh carbon was not commercially available, larger carbon was crushed and screened for use during testing
- De-ionized rinse water used to wash carbon between experiments

Basically, known reactant concentrations were passed through the reactor, within which the carbon particle size could be varied, and the amount of Fe(II) regenerated was measured in the effluent. From the known flow rate through the reactor, the solution volume within the reactor, and the measured change in Fe(II), the rate of regeneration was calculated. Desired test conditions (i.e., carbon particle size, flow rate and reactant concentrations) were determined from the testing protocol as described in the Design section below. A general schematic of the experimental process flow is shown in Figure 2.4 and a description is as follows:

1. electrolyte (mixed and heated to desired acid, iron and copper concentrations and temperature) was pumped from the mix tank at a known flow rate;
2. SO_2 was injected into the electrolyte flow at a known rate satisfying desired feed concentration, dissolving to aqueous form, before entering the Fe(II) regeneration reactor; and
3. feed flowed through the reactor, where Fe(III) was reduced to Fe(II), and the effluent was sampled for comparison to the feed.

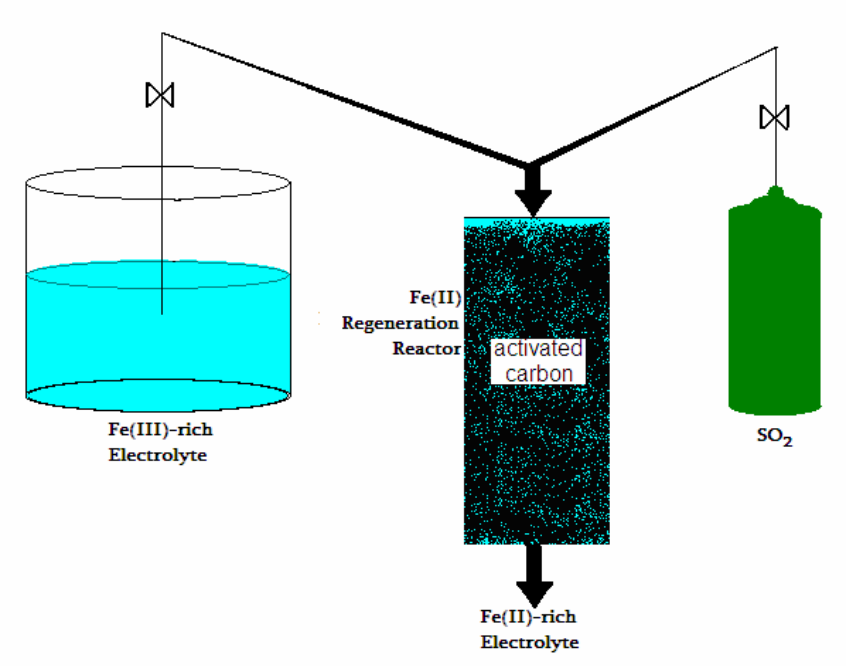

Figure 2.4 – Process Flow for Experimental Fe(II) Regeneration

Design

Data was collected during experiments with varied carbon particle size, flow rate (retention time) and Fe(III) and SO_2 concentrations. The test matrix was designed such that only one factor was varied at a time and there were a total of 45 experiments, including several replicates to determine the degree of data reproducibility. Temperature and acid, total iron and copper concentrations were maintained at constant values, which are given in Table 2.1 together with the variable ranges.

Table 2.1- Experimental Parameters

Varied Process Factors	Range
Mean Carbon Particle Size	499, 649, 843 µm
Flow Rate	80 - 390 mL/min
Fe(III) Concentration	1.0 - 10.0 g/L
SO_2 Concentration	0.3 - 3.0 g/L
Constant-value Parameters	**Value**
Temperature	120 °F
H_2SO_4 Concentration	160 g/L
Total Fe Concentration	30 g/L
Cu(II) Concentration	38 g/L

Temperature and acid concentration were kept constant for the reasons discussed previously in the model development section. Total iron concentration was kept constant at the stated concentration, since this is what would be experienced in commercial EW electrolytes for AART using FFS; the Fe(II) and Fe(III) ratio is varied by how much iron is reacted at the anode and how much is converted during the regeneration process. Similarly, copper was included in the electrolyte solution – also at a typical commercial concentration – since it is inherent to the EW process, and, hence, the Fe(II) regeneration aspect of AART using FFS. Although specific studies have not been conducted with respect to the effects of copper concentration, it has not been observed, nor is it expected, to significantly influence the regeneration.

Procedure

The experimental procedure should be prefaced with the following notes. First, the carbon used during experimentation was soaked in de-ionized water for at least one day prior to its use. Additionally, the same carbon was used for each experiment for which it was the correct size because the activity was assumed not to decrease significantly during experimentation, as has been observed in previous studies (Thomas and Ingraham, 1963). Since there were three carbon sizes tested, there were three volumes of carbon used during experimentation. After the carbon had been soaked, solution volume within the carbon was determined experimentally for use in calculating residence times. Finally, the density was determined for each volume of carbon (one for each of the three tested size classes) to be used during experimentation.

Since the experimental apparatus allowed for direct changes in electrolyte and SO_2 flow rates, flow rates were varied during testing and, then, converted to residence time values since the carbon volume and, hence, the solution volume within it, was fixed. Just before each experiment, reagent grade chemicals were measured to make electrolyte to concentrations per the test design protocol, and allowed to heat and mix for approximately one hour. When completely mixed and at the desired temperature, 120 °F, the reactor was operated, and data were collected:

1. An initial sample of the electrolyte was taken from the mix tank just before each experiment to use as a baseline for comparison with the effluent sample(s). Comparison with this sample negated concentration errors due to evaporation or measurement mistakes when mixing electrolyte.
2. About 2 L of de-ionized water was pumped through the carbon column to rinse any residual electrolyte or SO_2 from previous experiments. Then, about 2 L of the freshly mixed electrolyte was pumped through the column, or more, until the temperature of the column reached the desired temperature.
3. The electrolyte pump was set to the flow rate corresponding to the residence time called for by the test protocol, allowed to reach equilibrium, and verified by manual measurement.
4. Once the electrolyte had reached a desired constant flow, the SO_2 flow was started and set at a rate calculated to give the desired SO_2 concentration for a given experiment.
5. Based on the feed flow to the column, after enough time had elapsed for the reaction to come to equilibrium (about five residence times), a sample was taken from the effluent and allowed to cool. Particularly if the ratio of SO_2 to Fe(III) tested was high, the samples were capped and shaken, then uncapped and exposed to air several times to ensure that most of any SO_2 in solution was released.

The cooled initial and effluent electrolyte samples were analyzed for Fe(II) and total iron content. Measurements on each sample were completed in duplicate, and results were averaged to better ensure the accuracy of the data. Corrections, if necessary, were made for evaporation, and the initial Fe(III) concentration was determined to verify that it reasonably matched the test protocol. The amount of Fe(II) produced by the regeneration process was then determined as the difference between the concentrations in the initial and effluent samples, and converted to a rate value given the residence time for the experiment. The titration and AA methods described below were utilized for all samples, and, periodically, some sample duplicates were sent to another lab for verification.

Analytical Methods

To determine the change in Fe(II) concentration during the regeneration process for each experiment, a Fe(II) titration was completed on un-reacted and reacted electrolyte samples using potassium permanganate ($KMnO_4$) as the titrant. This titration method is rather common for Fe(II) and well documented (ASM, 1994). All titrations were done using a Metler-Toledo DL50 auto-titrator, which was regularly calibrated and standardized, before use and between about every 12 samples. Additionally, atomic absorption spectrometry (AA) was used to determine total iron concentration in all samples for two purposes. First, total iron measurement served as a method of checking and validating initial Fe(III) concentrations, i.e., Fe(III) is the difference between the total iron and Fe(II) concentrations. Second, these measurements were helpful in determining whether evaporation during testing was significant, i.e., if total iron concentrations were elevated in the effluent, then evaporation had to be considered. AA analysis is a common technique for measuring many types of metal ion concentrations in solution (ASM, 1992). A Perkin Elmer 1100 AA, was used and was also calibrated regularly. Finally, some sample duplicates were taken and sent to an outside lab throughout the testing to periodically verify titration and AA results; the other laboratory also used titration and AA to determine Fe(II) and total iron, respectively.

Results and Discussion

The Fe(II) regeneration rate data have been compiled and summarized to show the variables for each experiment – mean carbon particle size (and corresponding density), flow rate and initial concentrations of Fe(III) and SO_2 – and the resulting Fe(II) regeneration rate. A portion of the data summary is shown below in Table 2.2, and a full version is given in Appendix A (Table A.1).

Table 2.2 – Portion of Experimental Data Summary

Experiment	Mean Carbon Particle Size	Carbon Density	Flow rate	Initial Fe(III) Concentration		Initial SO_2 Concentration		$\frac{dFe^{2+}}{dt}$ observed
#	µm	g/cm^3	mL/min	g/L	mol/L	g/L	mol/L	mol/L-min
a1	843	1.24	80	0.60	0.011	3.00	0.047	0.0039
a2	843	1.24	80	0.60	0.011	3.00	0.047	0.0041
a3	843	1.24	125	0.90	0.016	0.75	0.012	0.0120
b1	649	1.26	188	1.42	0.025	0.75	0.012	0.0225
b2	649	1.26	220	3.88	0.069	0.75	0.012	0.0328
b3	649	1.26	230	4.06	0.073	1.00	0.016	0.0314
c1	499	1.33	194	2.46	0.044	1.00	0.016	0.0246
c2	499	1.33	230	4.07	0.073	1.00	0.016	0.0351
c3	499	1.33	272	4.48	0.080	0.75	0.012	0.0497

A total of six points were removed from the data set due to suspected errors either in experimentation (e.g., excessive SO_2 escape from the reactor) or in assay analyses (i.e., the measured Fe(II) product was higher than theoretically possible).

The assumption that initial SO_2 concentration is insignificant to Fe(II) regeneration kinetics under the tested conditions was confirmed by fitting the orders of each reactant to the experimental data, using the generalized rate expression given in Equation 10. A complete description of this exercise is presented in Appendix B (Part 1). The order of Fe(III) was about one (i.e., $x = 1$), as expected for a mass transfer reaction, and that of SO_2 was nearly zero. Therefore, Equation 12 was validated, and the Fe(II) regeneration rate can be expressed as a function of only the limiting reactant concentration, Fe(III). For each carbon size, the regeneration rate was plotted as a function of initial Fe(III) concentration (Figure 2.5); the solid lines represent linear trend-lines for the regeneration rate, and the points represent the experimental data.

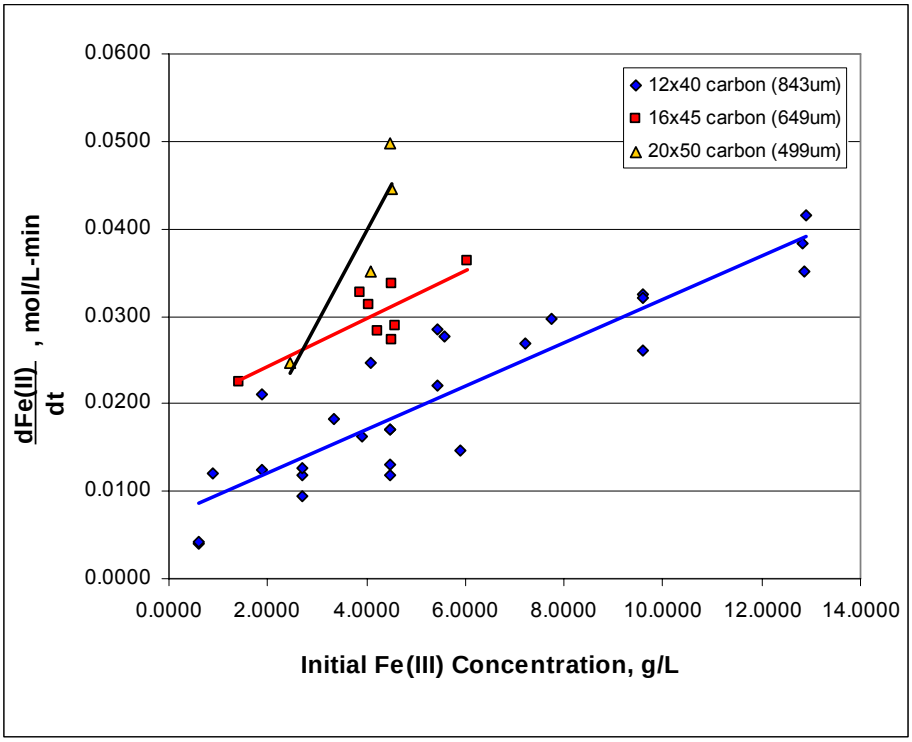

Figure 2.5 – Fe(II) Regeneration Rate as a Function of Initial Fe(III) Concentration

The faster regeneration rate with smaller carbon particles is as expected. Furthermore, the slopes of the trend-lines are the apparent rate constants, *k'*, which are clearly dependent on carbon particle size. The *k'* values obtained with the 12x40, 16x45, and 20x50 mesh carbon sizes are 0.0025, 0.0027 and 0.0105 mol/L-min, respectively. The regeneration rate values calculated with Equation 12 using the above *k'* values are listed in Appendix A (Table A.2) and compared to the observed values.

To better fit the experimental data, the rate model should include a rate constant that is explicitly a function of process factors other than reactant concentrations (e.g., carbon particle size and flow rate). This way, a single expression for the rate constant can capture variable conditions that affect the modeled process. As such, the general rate model was expanded to the hypothesized mass transfer model (Equation 17). Since the regeneration rate was determined to be first-order, the only unknown quantity was the diffusion coefficient of Fe(III), D_f. The diffusivity of a species is dependent on fluid flow in a system. Han (1990) determined a Fe(III) diffusion coefficient of 3.5×10^{-6} cm^2/s in a batch stirred reactor; however, the Fe(II) regeneration occurs within a continuously flowing system, so the Fe(III) diffusivity is lower. From Equation 17, a D_f value of 1.1×10^{-7} cm^2/s was found to best fit the experimental data. A complete discussion of the determination of the Fe(III) diffusion coefficient is given in Appendix B (Part 2).

Verification of the mass transfer model, and essentially that the Fe(II) regeneration rate is limited by the rate at which Fe(III) is transported to the carbon surface, was established by comparing the model predicted rate values to those observed during experimentation. A few points were removed from the data set because the experiments used to generate the points utilized Fe(III) concentrations or flow rates outside of their operable ranges for the current Fe(II) regeneration process. Such conditions were observed to produce results dissimilar to those produced when utilizing moderate Fe(III) concentrations and flow rates. This topic is also discussed in depth in Appendix B (Part 2). For all data collected under operable conditions, the experimental regeneration rate values were plotted against the model predicted values, as show in Figure 2.6. Data are listed and compared in Appendix A (Table A.2).

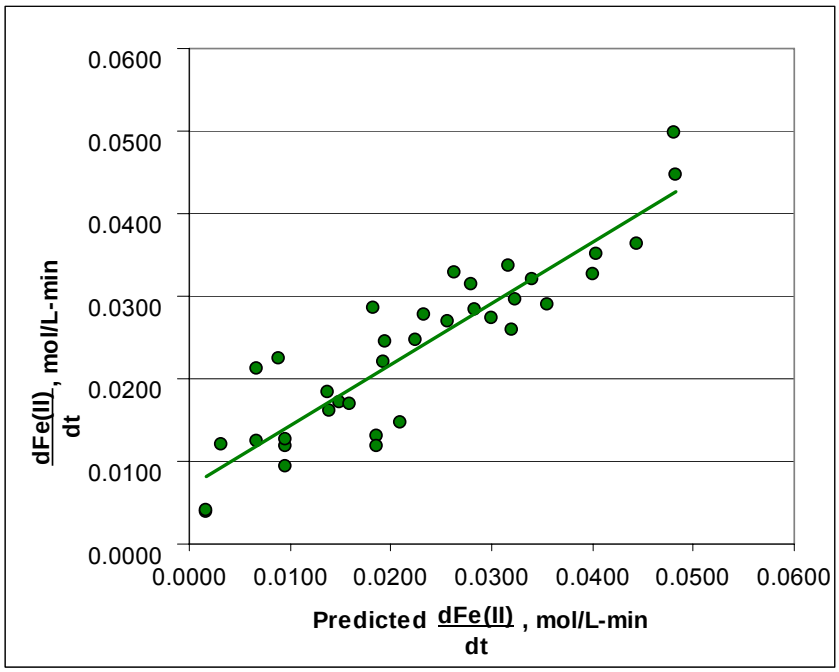

Figure 2.6 – Experimental Fe(II) Regeneration Rate vs. Mass Transfer Model Prediction

Overall, the mass transfer model correlates well to the experimental data. All but eight data points fit within 25% of the predicted model values, with roughly the same number of points above and below the model predictions. A perfect correlation would result in a trend-line with a slope of 1.0; the slope of the line in Figure 2.6 is 0.75. In view of the various flow rates being used, and the effect of flow rate on diffusivity, this correlation is excellent. Further evaluation of the model fit with respect to the tested carbon sizes is included in Appendix B (Part 3).

Finally, a comparison between the general Fe(II) regeneration rate model (Equation 12) and the mass transfer model (Equation 17) shows the significance of considering the rate mechanism in the kinetic model. Since the general rate constant, *k'*, has not been explicitly defined as a function of any process variables, a single, constant value should be used to compare the rate values predicted by the general and mass transfer models. As such, the general rate model utilizes a single, best-fit *k'* value, 0.047 mol/L-min, for the entire set of data points. The mass transfer rate constant, $\frac{6M}{\rho dV}[k_m]$, explicitly varies with several factors,

most importantly carbon particle size and flow rate (via slip velocity). In Figure 2.7, both the slope of the trend-lines and closeness of data points to them indicate the relative model fits.

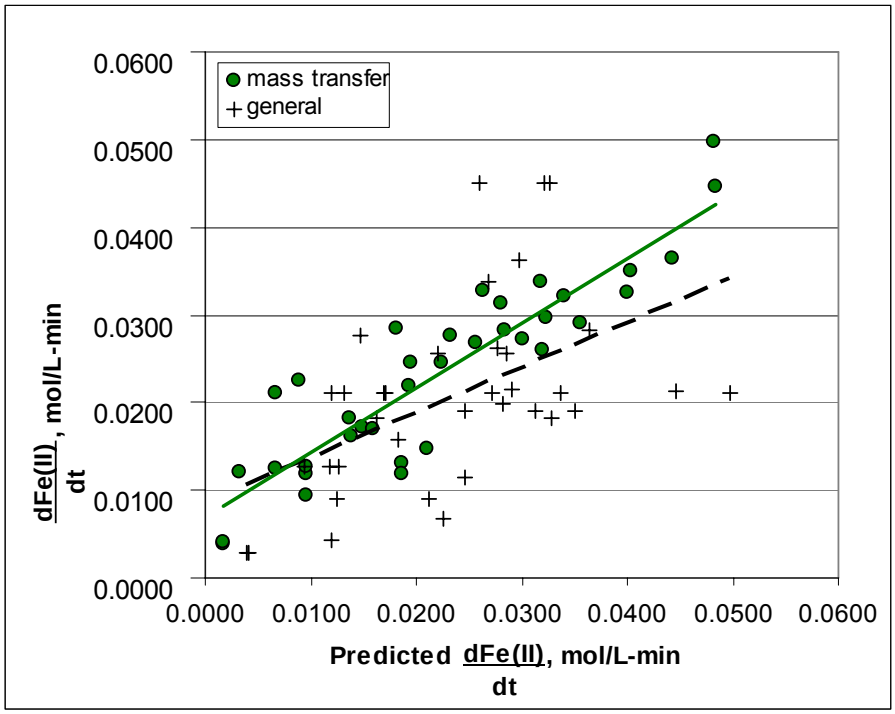

Figure 2.7 – Experimental Fe(II) Regeneration Rate Values vs. Rate Models

The general model has a slope of 0.52 and an R^2 value of 0.26, compared to the mass transfer model slope of 0.75 and an R^2 value of 0.82. Inclusion of the mass transfer factors, carbon particle size, diffusivity, flow rate and kinematic viscosity, results in both improved accuracy and precision of the Fe(II) regeneration rate model.

Conclusions and Recommendations

The Fe(II) regeneration process is an important aspect of AART using FFS for copper hydrometallurgy; however little has been done to study it specifically. SO_2 has been chosen as the most attractive oxidant for use in the process and, because the homogenous reaction between Fe(III) and SO_2 in solution is very slow, activated carbon is utilized as a surface catalyst. Although several factors may affect the regeneration reaction, few may be varied due to its place within the scheme of the entire hydrometallurgical process. The current work examined the effects of four variable factors – carbon particle size (i.e., surface area), flow

rate and the initial concentrations of the reactants, Fe(III) and SO_2 – with the purpose of developing a fundamental kinetic model for the Fe(II) regeneration.

A fundamental rate expression was derived from principles of chemical reaction rates and mass transfer phenomena, and a series of experiments were conducted to collect data that captured the effects of above factors. The following statements can be made about the Fe(II) regeneration under the tested conditions:

- A mass transfer rate model predicts the Fe(II) regeneration rate more accurately and precisely than a general model, which does not account for the reaction mechanism.
- The reaction rate is first-order, and is limited by the rate at which Fe(III) diffuses onto the carbon particle surfaces.
- Initial concentration of $SO_{2(aq)}$ does not significantly affect the reaction rate.
- The reaction rate is significantly increased by increased initial Fe(III) concentration or decreased carbon particle size.
- Flow rate significantly affects the diffusivity of a species; as a result, reaction rate is inhibited at very high flow rates.

The experimental data supported the hypothesized mass transfer rate model very well, especially within the currently operable ranges of initial Fe(III) concentration and flow rate. The finalized kinetic model for the Fe(II) regeneration rate (in mol/L-min) is of the following form, where D_f has a value of 1.1×10^{-7} cm^2/s:

$$\frac{dFe^{2+}}{dt} = \frac{6M}{\rho dV}\left[\frac{2D_f}{d} + 0.6\frac{V_t^{1/2} D_f^{2/3}}{d^{1/2}\nu^{1/6}}\right][C_{Fe^{3+}}]$$

It should be noted that the order, x, has been dropped from the above model equation since the regeneration was found to be first-order.

Furthermore, several recommendations can be made regarding additional test-work pertinent to the Fe(II) regeneration or similar reactions. First, the model might be validated within a wider range of variable factors by performing more tests designed with the results of the current work in mind. Such designs might quantify the effects of some process factors on

model terms, for example, the extent of the effects of flow rate on diffusivity. Second, the effect of temperature should be studied. Finally, the effects of carbon type and activity, including the change in activity with time and use, may be useful for commercial Fe(II) regeneration processes.

Chapter 3: An Empirical Optimization of the Current Ferrous Regeneration Process for Alternate Anode Reaction Technology

Emily Allyn Sarver

Abstract

The Fe(II) regeneration process is an important aspect of Alternate Anode Reaction Technology (AART) using a Fe(II)/Fe(III)-SO_2 (FFS) for copper hydrometallurgy. The process is basically Fe(III) reduction by $SO_{2(aq)}$, which is catalyzed by activated carbon particles. The current work examines the effects of four variable factors – carbon particle size, temperature, and initial Fe(III) and SO_2 concentrations – on the Fe(II) regeneration rate, followed by an optimization to maximize the rate. A requirement of negligible or no SO_2 in the process effluent is an added constraint on the rate, imposed by concerns for consequences of SO_2 in processes subsequent to the regeneration. Using Design Expert software to analyze and model the experimental results, carbon particle size and initial Fe(III) are the most influential of the tested factors, related to the rate linearly. Temperature is related to the rate by a squared term. Also, it is included in the model expression as a two-factor interaction with initial SO_2 concentration, although this term is the least significant. Optimization of the Fe(II) regeneration rate model results in the following combination factors over their tested ranges: minimum carbon particle size, maximum initial Fe(III) concentration, and moderate values of temperature and initial SO_2 concentration.

Introduction

Copper is currently the third most used metal in the world, primarily because of its exceptional electrical conductivity and resistance to corrosion. In 2003, about 17 million metric tons of copper were produced to supply the growing global demand (ICGS, 2003). In addition to increasing demand, copper prices have also been on the rise, skyrocketing to over $1.50 per pound in April 2005, up from just $0.68 only two years earlier (LME, 2005). Rising prices are due in part to growing production costs, which are not expected to decline to previous levels when energy was less expensive. High prices present a real advantage to low-cost producers, and new technologies that are capable of cutting costs are under serious consideration by the copper industry. One such technology – alternate anode reaction technology (AART) – has shown potential for a major reduction in power consumption, a primary cost center for electrowinning (EW) in hydrometallurgical production of copper (Sandoval and Lei, 1993; Sandoval et al., 1995; Sandoval and Dolinar, 1996).

AART basically changes the conventional EW anode reaction from water oxidation to ferrous [Fe(II)] to ferric [Fe(III)] iron oxidation, while the cathode reaction remains the same. This change results in two major advantages over the conventional process: substantial reduction in overall energy (power) requirements for EW and elimination of hazardous acid misting. The power reduction can be attributed to the reduced equilibrium potential of the alternate anode reaction, and the elimination of acid misting to the absence of O_2 production at the anode, which is present with the conventional anode reaction. One major aspect of the above AART is the necessity of Fe(II) regeneration – reducing the Fe(III) produced at the anode back to Fe(II) – to maintain recyclable EW electrolyte streams.

The method of regeneration that has been most successful during testing is Fe(III) reduction by SO_2. This method is attractive because SO_2 can be potentially obtained from nearby copper smelters, relatively easily and inexpensively. Also, the use of SO_2 as the reducing agent produces recoverable sulfuric acid as a by-product, which is beneficial because the acid may be utilized in leaching operations or sold (Sandoval and Dolinar, 1996). The combination of the Fe(II)-Fe(III) anode reaction and the subsequent Fe(II) regeneration

by SO_2 is abbreviated FFS. The FFS electrode reactions for copper EW and the Fe(II) regeneration reaction are shown below in Equations 1-4.

Anode reaction: $2 \times (Fe^{2+} \rightarrow Fe^{3+} + e^{-})$ (1)

Cathode reaction: $CuSO_4 + 2e^{-} \rightarrow Cu^{0} + SO_4^{2-}$ (2)

Overall EW reaction: $CuSO_4 + 2Fe^{2+} \rightarrow Cu^{0} + SO_4^{2-} + 2Fe^{3+}$ (3)

Fe(II) regeneration reaction: $SO_2 + 2Fe^{3+} + 2H_2O \rightarrow 2Fe^{2+} + SO_4^{2-} + 4H^{+}$ (4)

As can be seen above, for every mole of plated copper (Cu^0), two moles of Fe(III) are generated at the anode and must be reduced back to Fe(II) by a mole of SO_2. In practice, the SO_2 is injected into the Fe(III)-rich electrolyte after it leaves the EW cells, and then the solution is passed through a bed of activated carbon where the regeneration reaction occurs, shown in Figure 3.1. The role of the activated carbon is as a catalyst, which is discussed below. The recoverable acid by-product is produced when the excess H^+ in Equation 4 reacts with the copper sulfate ($CuSO_4$) already contained in the electrolyte.

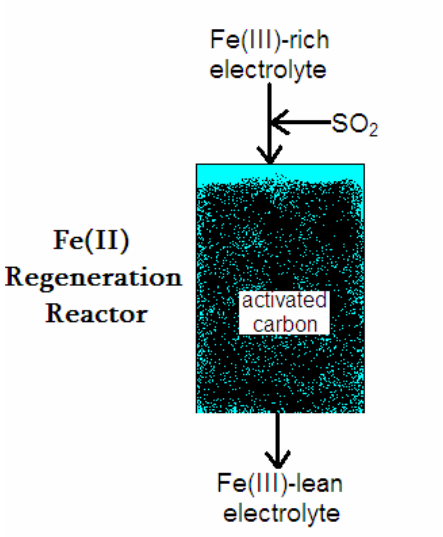

Figure 3.1 – Fe(II) Regeneration Reactor for AART Using FFS

Although the Fe(II) regeneration process has been successfully managed during both bench and pilot scale testing of AART using FFS, little has been done to study it specifically. For commercial operation, a better understanding of which process factors affect the regeneration, and in what ways, may assist in process design or improvement with respect to

the process parameters, circuitry, equipment or materials. To relate process factors to results, an optimization problem was defined and solved. First, process constants, variable factors and their operable ranges, and desirable responses were defined. Then, a series of experiments were conducted to determine the combination of variable factors that, under fixed conditions, will produce the most desirable results.

Literature Review

An understanding of the Fe(II) regeneration process parameters is essential to developing and solving the optimization problem. Due to its place within the scheme of EW, and the entire hydrometallurgical process including leaching and solvent extraction, many of the regeneration process parameters are fairly fixed. Acidity and copper concentration, for instance, cannot be varied without changing many other processes, while parameters specific to the regeneration process, like temperature and catalyst properties, might be adjusted rather easily. Other factors, such as iron and SO_2 concentrations, might be varied within certain ranges such that subsequent operations will experience small or negligible effects. For example, the Fe(III) concentration might be varied somewhat, but it must be kept in certain proportion with Fe(II) in the EW cells to maintain high current efficiency. Likewise, SO_2 concentration might be varied within its potential range of consumption by the Fe(II) regeneration reaction, but if it is varied considerably outside of this range the regeneration will not be efficient or un-reacted SO_2 could escape during EW, a hazardous consequence.

A review of the regeneration and similar processes provides some insight into reaction mechanisms and influential factors. The homogeneous Fe(II) regeneration reaction has been observed to be slow occurring in solution, a fact documented by Sandoval and Dolinar in a 1996 study of AART using FFS. Similar observations have been made of both of the half-reactions associated with the regeneration, Fe(III) reduction and SO_2 oxidation, when studied separately (Kumar et al., 1996; Govindarao and Gopalakrishna, 1995; Garcia et al., 1998; Thomas and Ingraham, 1963; Seaburn and Engel, 1993; Komiyama and Smith, 1975; Berglund et al., 1993). When catalyzed by a solid complex, such as activated carbon or graphite, the rates of such reduction-oxidation reactions have been shown to increase by up to three orders of magnitude (Thomas and Ingraham, 1963). Sandoval and Dolinar noted

a dramatic increase in the Fe(III)-SO_2 reaction rate when they tried catalyzing the reaction by passing the electrolyte containing the reactants through a bed of activated carbon, although the enhanced performance was not quantified. Several mechanisms have been suggested for reduction-oxidation reactions catalyzed by solid surfaces, most commonly surface adsorption and electron transfer phenomena; however, the behavior of each reactant, and other non-reactive species, and the reaction responses to various factors are typically quite specific to the process in question (Kumar et al., 1996; Govindarao and Gopalakrishna, 1995; Garcia et al., 1998; Thomas and Ingraham, 1963; Komiyama and Smith, 1975; Berglund et al., 1993). In a 1998 study by Garcia et al., the proposed mechanism included a heterogeneous reaction, whereby the oxidant adsorbed onto the catalyst surface and reacted with the reducing agent still in solution. Despite differing degrees of catalysis, a connection can generally be made between surface area and reaction responses, so catalyst surface area will clearly be a factor in the Fe(II) regeneration process.

Additionally, solid-surface catalyzed reduction-oxidation reactions involving iron ions and/or S(IV) species have been observed to be affected by several other variables (Sandoval and Lei, 1993; Kumar et al., 1996; Govindarao and Gopalakrishna, 1995; Garcia et al., 1998; Thomas and Ingraham, 1963; Seaburn and Engel, 1993; Komiyama and Smith, 1975; Krissman et al., 1998; Berglund et al., 1993). Typically, increased temperature has been observed to have a positive effect on reaction rate, while things like acidity and adsorption of non-reactive species have tended to inhibit reactions. In batch tests, non-reactive species have even been determined to deactivate the catalyst by blinding potential adsorption sites from reactive species (Kumar et al., 1996; Govindarao et al., 1995). However, in continuous flow tests using activated carbon as a catalyst, the activity has been observed to be long-lasting in the presence of similar iron and acid concentrations as are common for EW electrolytes (Thomas and Ingraham, 1963).

Concentrations of reactants and non-reactive species have been observed to influence solid-surface catalyzed reactions differently, specific to the reactants, products and reaction mechanism(s). As stated above, if the non-reactive species adsorb onto the catalyst and are retained, they can have a mild to severe deactivating effect. They might also assist or be

insignificant in the reaction, as was observed of Cu(II) ions by Kumar et al. in a 1996 study of SO_2 oxidation by dissolved O_2. As well, one reactant may dominate the reaction if, for example, it adsorbs onto the catalyst surface much faster than another reactant or is present in relatively large concentrations. Reaction products can also affect reaction progression if they aid or inhibit it in any way. For instance, in the aforementioned Garcia et al. study, the rate of Fe(III) reduction was slowed by the production of Fe(II) when the Fe(II) adsorbed onto the graphite catalyst and prevented further adsorption of the reacting species. The affects of solution constituent concentrations for the Fe(II) regeneration will depend on reaction stoichiometry, mechanism(s) and the continuous flow nature of the process.

Optimization Problem Development

To set up the optimization problem, process constants, variable factors and their operable ranges, and desirable responses were defined.

Particular to the current regeneration process, several fixed conditions are present which may certainly affect it: electrolyte acid, total iron and copper concentrations. Due to the relatively high acidity, when SO_2 is dissolved into the electrolyte the predominant species will be $SO_{2(aq)}$, which is known to react slower than bisulfite (HSO_3^-), the predominant species at lower acidity (Kumar et al., 1996; Govindarao and Gopalakrishna, 1995; Garcia et al., 1998; Krissman et al., 1998). Also, Fe(II), either initially in the electrolyte or produced by the regeneration reaction, could inhibit the progression of the regeneration if it prevents adsorption of reactants onto the catalyst. In the range of concentration for the regeneration process, such inhibition does not appear likely considering published diffusivity data that suggests SO_2 will adsorb onto the catalyst faster than iron ions (Han, 1990; Freiberg and Schwartz, 1981; Ramsing and Gundersen, no date given). Conversely, if the copper concentration has any effect it will likely interfere as a catalyst for the homogeneous reaction rather than as an inhibitor, as has been proposed in previous studies of similar reactions (Kumar et al., 1996). Although these conditions may play a role in the regeneration, they are fixed within the current process and will be maintained as constant parameters for the purpose of optimization.

Considering these constants, the regeneration reaction and the findings of previous studies surrounding similar reactions, the (variable) influential process factors and their operable ranges were identified. The factors are activated carbon surface area, temperature, and reactant – Fe(III) and SO_2 – concentrations. Carbon surface area can be easily varied without affecting other operations, the most problematic issues being carbon containment within the reactor (e.g., if particles are too small, they will either wash through containment mesh at the bottom of the reactor or the mesh will be so tight that it inhibits flow) and obtaining odd sized carbons (i.e., sizes not commercially available). Temperature can also be varied fairly easily, although excessive temperature changes could present large costs in time and/or money. Fe(III) concentration can be varied somewhat; since total iron is constant, varying Fe(III) means varying Fe(II) equally but oppositely. In order to increase Fe(III) concentration, more Fe(II) must be oxidized at the anode and this is limited by concern for EW efficiency (i.e., Fe(II) is depleted in the EW cells, so increased oxidation requires more time or voltage and thus reduces efficiency). Finally, SO_2 can be varied with Fe(III) concentration such that the two are within the proper proportions for the regeneration reaction, which depend on both stoichiometry and the extent of the reaction. It is important to achieve a complete reaction (i.e., prevent un-reacted SO_2) while regenerating as much Fe(II) as possible, precisely the conditions of the optimization, as discussed below. Considering how each factor might be varied and their values during previous successful Fe(II) regeneration within AART using FFS testing, an operable range was defined for each process factor. Ranges are shown in Table 3.1 along with the constant process parameters and their respective values for the optimization.

Table 3.1 – Experimental Parameters

Varied Process Factors	Low-Value	Mid-Value	High-Value
Fe(III) Concentration	2g/L	4g/L	6g/L
SO_2 Concentration	0.50g/L	0.75g/L	1.00g/L
Temperature	110°F	120°F	130°F
Mean Carbon Particle Size	499μm	649μm	843μm
Constant-value Parameters		**Value**	
H_2SO_4 Concentration		160g/L	
Total Fe Concentration		30g/L	
Cu(II) Concentration		38g/L	

As is often the case, the main goal of the optimization problem for the current Fe(II) regeneration process was to maximize throughput. Since the process reaction is essentially contained within fixed volume reactors, maximum throughput occurs at the minimum residence time of electrolyte within the reactor(s) because the two quantities are inversely related, as shown in Equation 5, where F is electrolyte throughput or flow, V is electrolyte volume in the reactor, and τ is residence time.

$$F = \frac{V}{\tau} \tag{5}$$

Additionally, two conditions on this goal had to be considered for regeneration efficiency and safety: Fe(II) regeneration should be as high as possible in order to supply as much Fe(II) for the EW anode reaction as possible, and break-through (un-reacted) SO_2 in the reactor effluent should be as low as possible to avoid SO_2 escape when electrolyte is exposed to air (i.e., in the EW cells). These conditions are individually satisfied at process extremes. With excessive SO_2 supply to the regeneration reactor, the highest amount of Fe(II) will be regenerated but break-through SO_2 will occur; with minimal SO_2 supply, break-through SO_2 will be easily prevented but less Fe(II) will be regenerated.

Considering the above goal and conditions, criteria were established to measure the success of the Fe(II) regeneration process as the factors were varied over their respective ranges. First, process success only occurs if there is no (or negligible) break-through SO_2. Second, the optimal combination of process factors is the one that results in the minimum successful residence time at a maximum level of Fe(II) regeneration. For experimentation,

the criteria could be quantified by a single response to a particular combination of the process factors; the Fe(II) regeneration rate, $R_{Fe^{2+}}$, which could be calculated using Equation 6 where dFe^{2+} is the amount of Fe(II) produced at the minimum residence time, $\tau_{\min}$. By maximizing $R_{Fe^{2+}}$, the optimal ratio between Fe(II) regeneration and minimum residence time could be determined. The solution may be used to improve current operations or to design reactors and process conditions for future operations. $R_{Fe^{2+}}$ may be easily used in scale-up problems since the minimum residence time may be related to any number of reactor sizes (i.e., solution volumes) and feed flow rates.

$$R_{Fe^{2+}} = \frac{dFe^{2+}}{\tau_{\min}} \qquad (6)$$

During the experimentation described below, the process factors were empirically related to the responses and an optimization was completed.

Experimental

To collect data capturing the effects of carbon particle size, temperature and the initial concentrations of Fe(III) and SO_2 on rate of regeneration, a bench-scale Fe(II) regeneration reactor was constructed. The reactor was operated under similar conditions to a larger-scale process (e.g., temperature, acidity, Fe(II) to Fe(III) ratio). All test work was completed at the SX/EW Test Facility, operated by the Phelps Dodge Process Technology Center in Morenci, AZ.

Apparatus and Materials

The apparatus for Fe(II) regeneration experiments consisted of the following parts:

- 12” Plexiglas column from Waters Equipment (1.45” internal diameter) with top and bottom mesh-covered screw-caps fitted for electrolyte and effluent flows; when filled with activated carbon, the column functioned as the Fe(II) regeneration reactor
- 150 lb pressurized SO_2 tank with a digitally-set Porter Instruments mass flow controller rated for 0-150 mL/min flow
- 20 L electrolyte mix tank with variable speed mixer, and coil immersion heater with Cole Parmer Dyna-Sense controller

- Cole Parmer Masterflex automatic-dispensing electrolyte pump rated for 4-480 mL/min flow with digital controller
- Catch tank, tubing and fittings, valves and check valves, thermometer, stopwatch, 15 mL sample tubes with airtight caps

The apparatus is shown in Figure 3.2 below.

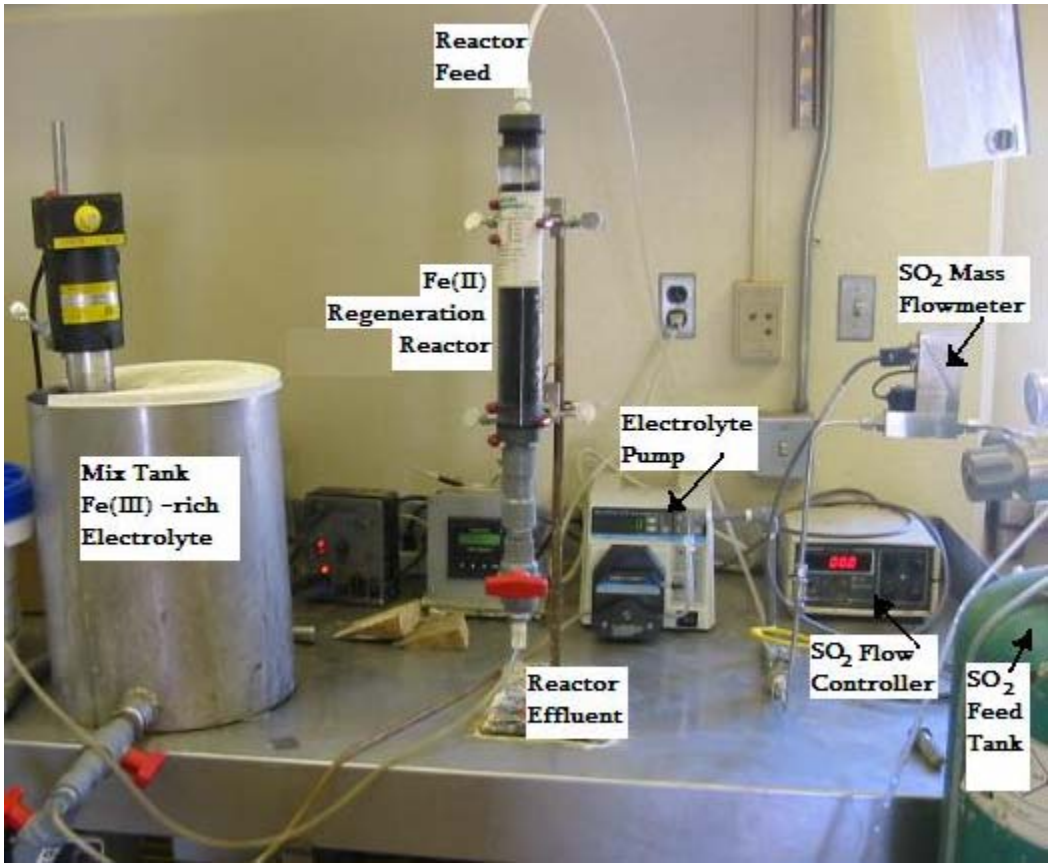

Figure 3.2 – Experimental Apparatus

Materials for the experiments consisted of the following:

- Electrolyte ingredients: reagent grade sulfuric acid (97%), ferrous (100%) and ferric (76%) sulfates, technical grade copper (II) sulfate (98%), and de-ionized water; reagent grade chemicals were obtained from chemical suppliers, Cole-Parmer and VWR, and the copper (II) sulfate was obtained from a Phelps Dodge refinery.
- Gaseous SO_2 (from pressurized tank)
- Activated carbon (of bituminous coal type) of three mesh class sizes: 12x40 (mean particle size 843 μm), 16x45 (mean particle size 649 μm) and 20x50 (mean particle

size 499 μm); carbon was obtained from TIGG, but as 16x45 mesh carbon was not commercially available, larger carbon was crushed and screened for use during testing

- De-ionized rinse water used to wash carbon between experiments

Basically, known reactant concentrations were passed through the reactor, within which the carbon particle size could be varied, and the amount of Fe(II) regenerated was measured in the effluent. From the known flow rate through the reactor, the solution volume within the reactor, and the measured change in Fe(II), the rate of regeneration was calculated. Desired test conditions (i.e., carbon particle size, flow rate and reactant concentrations) were determined from the testing protocol as described in the Design section below. A general schematic of the experimental process flow is shown in Figure 3.3 and a description is as follows:

1. electrolyte (mixed and heated to desired acid, iron and copper concentrations and temperature) was pumped from the mix tank at a known flow rate;
2. SO_2 was injected into the electrolyte flow at a known rate satisfying desired feed concentration, dissolving to aqueous form, before entering the Fe(II) regeneration reactor; and
3. the feed flowed through the reactor, where Fe(III) was reduced to Fe(II), and the effluent was sampled for comparison to the feed.

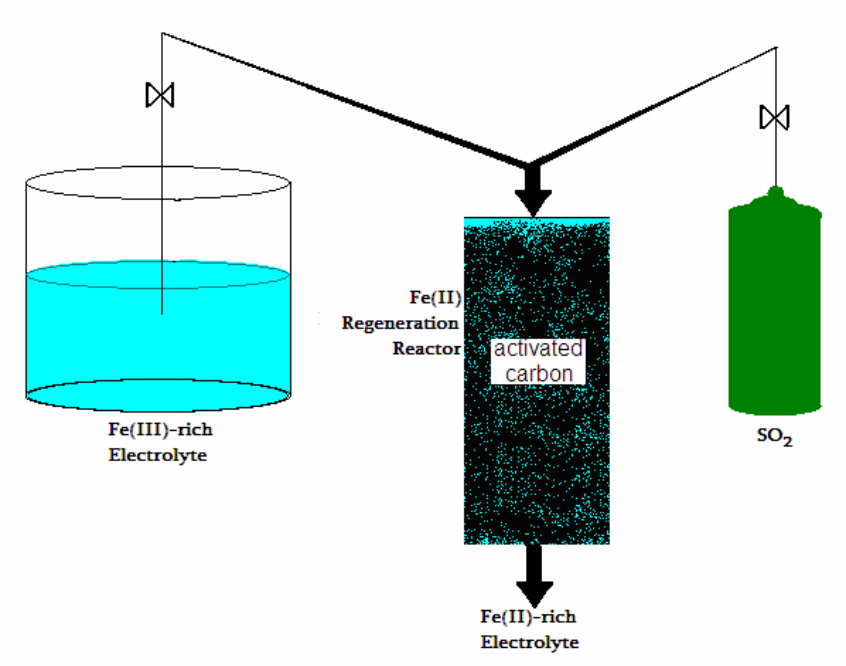

Figure 3.3 – Process Flow for Experimental Fe(II) Regeneration

Design

Experimental design, results analysis and optimization were completed using Design Expert 6.0, a software package by Stat-Ease with capabilities to relate multiple process factors and responses. Using a response-surface method and (face-centered) central composite type design, the four process factors (independent variables) were varied over three levels each in a set of 30 experiments, a sufficient number for creating a statistically significant model. This method and design type are ideal for optimization problems because experiments capture points on the interior and boundaries of the design space such that the model(s) generated are representative of the entire space. Subsequent optimization determines the combination of factor values within the design space that produces the desired response.

The testing protocol included six replicates on the center point of the design space, eight axial points and 16 factorial points in the 30-experiment set. The four numeric process factors and their respective operable ranges were as defined in Table 3.1. Particle size was characterized by the geometric mean size within a given class. Carbon particle size was modeled as a numeric factor so that during optimization the size could be indicated between

actually available sizes if preferred. The process response was Fe(II) regeneration rate at minimum residence time, as defined above. Each experiment was conducted at its particular combination of process factors, per the test protocol, and the response was measured per the procedure below.

Procedure

The experimental procedure should be prefaced with the following notes. First, the carbon used during experimentation was soaked in de-ionized water for at least one day prior to its use. Additionally, the same carbon was used for each experiment for which it was the correct size because the activity was assumed not to decrease significantly during experimentation, as has been observed in previous studies (Thomas and Ingraham, 1963). Since there were three tested carbon sizes, there were three volumes of carbon used during experimentation; after the carbon had been soaked, solution volume within the carbon was experimentally determined for use in calculating residence times. Finally, approximate flow rates were determined during a series of preliminary tests at various Fe(III) and SO_2 concentrations, such that maximum flow rate (minimum residence time) could be determined relatively quickly during each of the 30 experiments, as to avoid evaporation or critical depletion of the electrolyte feed.

For each experiment, a two-part procedure was conducted: determination of minimum residence time followed by determination of Fe(II) regeneration at the minimum residence time. Since the experimental apparatus allowed for direct changes in electrolyte and SO_2 flow rates, flow rates were varied during testing and then converted to residence time values since the carbon volume, and hence the solution volume within it, was fixed. The experimental procedure is described below.

Determination of Minimum Residence Time

Reagent grade chemicals were measured to make electrolyte to concentrations required by the test protocol just before each experiment, and allowed to heat and mix for approximately an hour. When completely mixed and at the desired temperature for a given experiment, the minimum residence time was determined:

1. An initial sample of the electrolyte was taken from the mix tank just before each experiment to use as a baseline for comparison with the effluent sample(s). Comparison with this sample negated concentration errors due to evaporation or measurement mistakes when mixing electrolyte.
2. About 2L of de-ionized water was pumped through the carbon column to rinse any residual electrolyte or SO_2 from previous experiments. Then about 2L of the fresh electrolyte was pumped through the column, or more until the temperature of the column reached the desired temperature for a given experiment.
3. The electrolyte pump was set to a conservative flow, one which allowed for a nearly complete reaction of initial Fe(III) and SO_2 concentrations required for a given experiment, and the flow rate was allowed to reach equilibrium, verified by manual measurement.
4. Once the electrolyte had reached a desired constant flow, the SO_2 flow was started and set at a rate calculated to give the desired SO_2 concentration for a given experiment.
5. Based on the feed flow to the column, after enough time had elapsed for the reaction to come to equilibrium (about five residence times), a sample was taken from the effluent and immediately capped. All samples were taken and analyzed for break-through SO_2 as stated below in the Analytical Methods section, and SO_2 readings and corresponding flow rates were recorded. If break-through SO_2 was determined to be present in the sample, the experiment was run at a slower flow rate; if SO_2 was not present, the flow rate was increased.

This procedure was repeated incrementally until the maximum flow rate could be determined within 10-20mL/min increments; minimum residence time was calculated from the maximum flow rate and solution volume within the carbon using Equation 5. Additionally, all SO_2-flow rate data were analyzed for each experiment with multiple data points to determine if a general trend could be established (i.e., how does break-through SO_2 change with flow rate?)

Determination of Fe(II) Regeneration

Upon determination of the minimum residence time for each experiment, the initial electrolyte sample and the effluent sample from the reactor when operated at the minimum residence time were analyzed for Fe(II), total iron and Cu(II) content. Measurements on each sample were completed in duplicate and results were averaged to better ensure the accuracy of the data. Corrections, if necessary, were made for evaporation, the initial Fe(III) concentration was determine to verify it reasonably matched the test protocol, and the amount of Fe(II) produced by the regeneration process was determined as the difference between the concentrations in the initial and effluent samples. The titration and AAS methods described above were utilized for all samples, and periodically some sample duplicates were sent to another lab for verification.

Analytical Methods

For determining minimum residence time, it was necessary to determine whether or not the reactor effluent contained break-through SO_2. Measurement of SO_2 in solution is possible via iodimetry, however this method was not feasible for the Fe(II) regeneration experiments for several reasons (e.g., lack of required materials, time constraints per the experimental procedure, and/or reliability of analysis by an outside party due to loss of SO_2 concentration). Since, per the two-part experimental procedure below, it was only necessary to find if SO_2 was present in the effluent, not an exact quantity, a hand-held gas monitor was used. The monitor was an Industrial Scientific T82 single gas monitor with an SO_2 sensor, which detected SO_2 gas in the range of 0.2-150ppm. The gas intake area on the monitor was lined with a rubber seal, which fit fairly tightly over the top of the 15mL sample tubes used during testing. Since the ppm reading was not an exact measurement but more of an SO_2 indicator, the following procedure was used to determine whether or not break-through SO_2 was present in a sample.

- A 15mL sample tube was filled to the 14mL mark with effluent directly from the reactor and immediately capped.
- The sample was allowed to sit and cool for 15 minutes. Due to the partial pressure of SO_2, if any was present, it would readily come out of solution and fill the 1mL space in the capped tube.

- The sample was uncapped and the SO_2 monitor was immediately fitted over it.

If the monitor read above 2ppm, the sample was considered to contain break-through SO_2; 2ppm or less was considered negligible. For the purposes of this paper, "minimum residence time" then refers to the shortest residence time allowing 2ppm or less of break-through SO_2. This method of SO_2 detection was quite conservative considering the sample and air volumes used and the current SO_2 allowances set by OSHA (PEL = 5ppm, TLV = 2ppm), (OSHA, 2005).

To determine the change in Fe(II) concentration during the regeneration process for each experiment, a Fe(II) titration was completed on un-reacted and reacted electrolyte samples using potassium permanganate ($KMnO_4$) as the titrant. This titration method is rather common for Fe(II) and well documented (ASM, 1994). All titrations were done using a Metler-Toledo DL50 auto-titrator, which was regularly calibrated and standardized, before use and between about every 12 samples. Additionally, atomic absorption spectrometry (AAS) was used to determine total iron and Cu(II) concentrations in all samples for two purposes. First, total iron measurement served as a method of checking and validating initial Fe(III) concentrations (i.e., Fe(III) is the difference between the total iron and Fe(II) concentrations). Second, both total iron and copper measurements were helpful in determining whether evaporation during testing was significant (i.e., if total iron and Cu(II) concentrations were elevated in the effluent, then evaporation had to be considered). AAS analysis is a common technique for measuring many types of metal ion concentrations in solution (ASM, 1992). It was completed using a Perkin Elmer 1100 AA, also calibrated regularly. Finally, some sample duplicates were taken and sent to an outside lab throughout the testing to periodically verify titration and AAS results; the other lab also used titration and AAS to determine Fe(II) and total iron, respectively.

Results and Discussion

For each experiment, individual data sheets were created containing the following information: test protocol values for process factors, initial and effluent electrolyte Fe(II), total iron and Cu(II) assays, and break-through SO_2 trends with changing flow rate (reactor

residence time). The effluent assays were only taken on samples from the minimum residence time test for each experiment. A sample data sheet is shown below in Figure 3.4.

date 14-Oct-04 Exp 15

TEST CONDITIONS								
given/required conditions	carbon volume	253.69	mL	measured from initial sample	Fe3+ conc.	6.18	g/L
	SO2 conc.	0.50	g/L		Total Fe conc.	30.72	g/L
	SO2 density	0.003017	g/cc		Fe2+ conc.	24.54	g/L
	outlet pressure	2.00	psi		Cu conc.	38.43	g/L
	atm pressure	14.70	psi		Acid conc.	159	g/L
	atm temp	294.00	K		solution temp	110	F

Parameter Settings			Measured Responses (Effluent					
electrolyte flowrate mL/min	SO2 flowrate cc/min	residence time min	SO2	Fe2+ g/L	Total Fe g/L	Fe3+ g/L	Cu g/L	Acid g/L
0.00	0.00	0.00	0	24.54	30.72	6.18	38.43	159
142.00	23.50	1.79	1.4	25.22	30.93	5.71	38.6	159.8
169.00	27.80	1.50	2.6					
183.50	30.40	1.38	3.3					
209.00	34.60	1.21	8					
238.00	39.50	1.07	12.6					

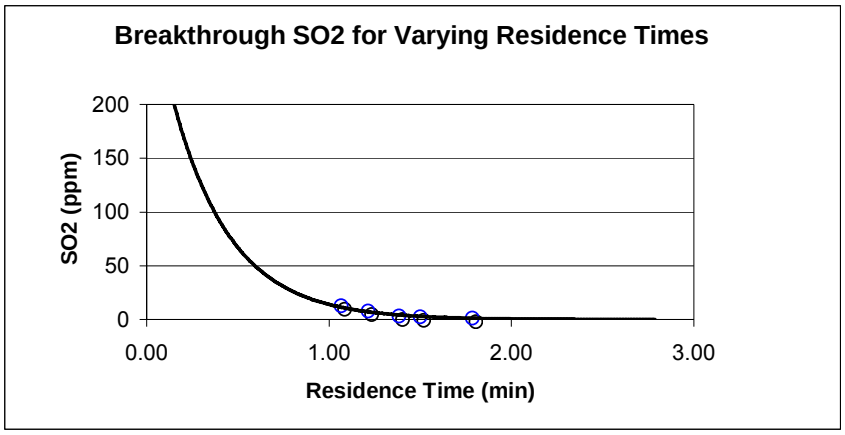

Figure 3.4 – Sample Data Sheet for an Individual Experiment

The data sheets like the one shown in Figure 3.4 were used to assess the trend of break-through SO_2 with flow rate, as well as compile an overall summary. For all experiments during which multiple flow rates were applied to determine the minimum residence time, a clear exponential trend was observed in break-through SO_2 with increasing flow rate. Although too few data were collected to quantify a relationship between the process factors and the exponential trend in break-through SO_2, the general trend is important. It indicates that if the Fe(II) regeneration process is operated at residence times

less than the minimum time, break-through SO_2 can become problematic very quickly. If a deeper understanding of this issue is required, more experimentation is necessary.

It should also be noted that while the experimental procedure appears to be capable of producing precise results, it is possible that some constant error may be associated with the experimental data due to inability to ensure a completely solution-filled reactor. SO_2 partially came out of the electrolyte solution to fill any air space at the top of the reactor for all of the experiments, which undoubtedly reduced the aqueous concentration available for the reaction. Since, due to set-up of the reactor, this phenomenon was unavoidable, an effort was made to control it by minimizing the air space. This way, the error could be kept relatively constant, except for small changes in how much SO_2 would come out of the electrolyte caused by varying temperature or flow rate.

From the individual data sheets, an overall summary was generated to include the following information for each experiment: process factor values, minimum residence times and corresponding flow rate, effluent Fe(II) assays and calculated Fe(II) regeneration rate, $R_{Fe^{2+}}$ (per Equation 6). A portion of the data summary is presented below in Table 3.2, and the entire summary is given in Appendix C (Table C.1).

Table 3.2 – Portion of Experimental Data Summary

Experiment	Process Factors				Process Responses		
	Initial SO_2 Concentration	Initial Fe(III) Concentration	Reaction Temperature	Mean Carbon Particle Size	Flow Rate	Minimum Residence Time	$\frac{dFe^{2+}}{t_{min}}$
#	(g/L)	(g/L)	(°F)	(μm)	(mL/min)	(min)	(mol/L-min)
1	0.50	4.6	116	649	292	0.523	0.0290
2	0.75	1.4	126	649	188	0.801	0.0225
10	0.75	4.0	126	649	314	0.480	0.0118
11	0.75	6.0	121	649	261	0.585	0.0364
14	0.50	2.8	130	843.5	156	0.974	0.0055
15	0.50	6.2	112	843.5	169	0.899	0.0101
19	1.00	2.0	128	843.5	106	1.434	0.0030
20	1.00	6.1	112	843.5	114	1.333	0.0151
24	0.50	6.3	109	499	336	0.454	0.0143
25	0.50	5.2	131	499	326	0.468	0.0218
28	1.00	2.1	134	499	204	0.748	0.0110
29	0.98	6.2	111	499	248	0.615	0.0255

Model Construction

The values for the process factors and Fe(II) regeneration rate response were loaded into Design Expert for analysis. While the experimental design was created as a central composite type, the data were analyzed based on a "historical" design. The only major difference between the two design types is that "historical" design type feature of the software allows entry of actual values for process factors; central composite designs only allow entry of test protocol values. Since some of the Fe(II) regeneration process factors, particularly initial Fe(III) concentration and temperature, could not be set exactly to the test protocol values for each experiment, analysis using the "historical" design accounts for slight variations. Additionally, the actual values were sufficiently close to the protocol values as to not compromise the significance of the model generated from the experimental data. Statistical measures including model prediction variance and correlation of the process factors (i.e., orthogonality of the design) remained satisfactory for the "historical" design as compared to the central composite type. Table C.2 in Appendix C shows major statistical measurements for both design types, and Table C.3 gives the complete "historical" design evaluation for the experimental data points by the Design Expert software.

Upon analysis of the experimental data by the software, a quadratic model with a logarithmic transformation was suggested as the model type for the best fit to the data. The complete fit summary, which highlights various model types (e.g., linear, quadratic, cubic) and how well they fit the data points, is included as Table C.4 in Appendix C. A natural log transformation with a constant, k, of zero was chosen for the model, meaning the $R_{Fe^{2+}}$ response was transformed as shown in Equation 7, such that the model response, R_{model}, is the natural log of $R_{Fe^{2+}}$.

$$R_{model} = \ln(R_{Fe^{2+}} + k) \qquad (7)$$

Using the above model type, Design Expert was able to model the Fe(II) regeneration experimental data significantly, meaning that variance could be explained by the relationship between model factors and the response, and was not likely due to noise. In fact, the statistical chance that the model variance could occur due to noise was only 0.01%.

Design Expert analyzed the fit of the model to experimental data using numerous statistical measures. In addition to assessing the model significance, the software evaluated the fit of the model within the design space, the variance in residuals and their normality, and the fit of individual data points and their relative influence on the model. A comprehensive summary of all model statistics (ANOVA) as calculated by Design Expert is given in Table C.5 in Appendix C, and below is a discussion of the major statistics.

The model signal was determined to be more than adequate to navigate the design space (i.e., the model should reasonably predict R_{model} for any combination of process factors within their tested ranges.) The predicted and adjusted R-squared values also indicated a good model fit, as they were 0.77 and 0.80, respectively. The predicted value is a measure of how well the model predicts a response; the adjusted value accounts for how much of the variance can be explained by the model, which was most of the variance as stated above. A "good" fit is statistically defined as R-squared values that are within about 0.20 of each other, which they were for the Fe(II) regeneration model.

As well, Figure 3.5 confirms that residuals (difference between the actual and model predicted) have a normal distribution. In the plot, the residuals have been studentized, meaning that they are basically a measure of the number of standard deviations between the actual and predicted values. (The studentized residual value is calculated from the quotient of the residual and the standard deviation of the residual.)

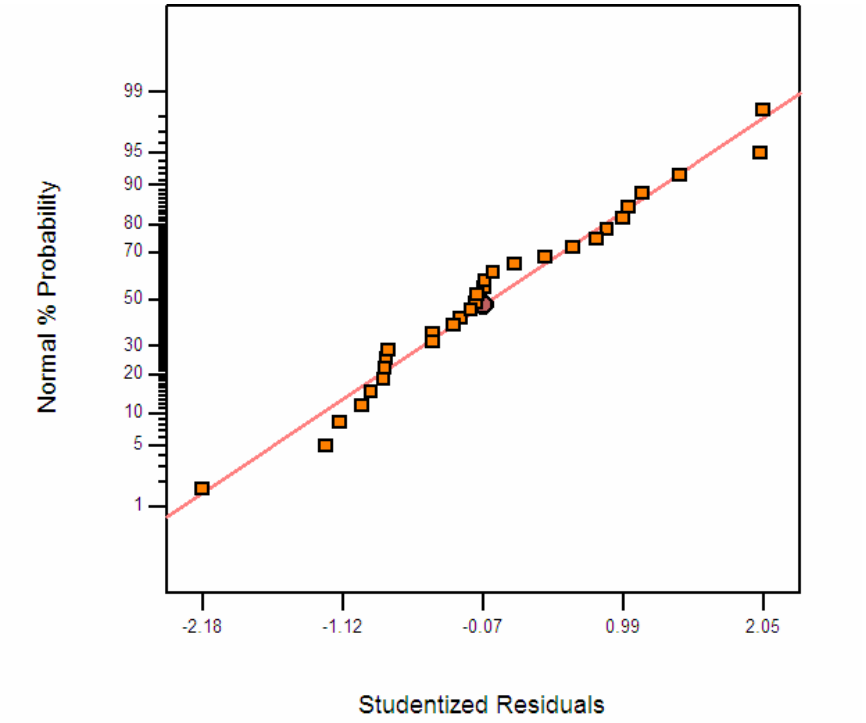

Figure 3.5 – Normal Plot of Residuals for Design Expert Model

To determine if any points should be considered statistical outliers, the "outlier T" value was calculated for each data point. This value shows how well a particular point fits within the rest of the data; values greater than 3.5 are considered extreme, and corresponding points should be removed from the data set as statistical outliers. From Figure 3.6, none of the 30 experimental data points have associated extreme "outlier T" values, so none should be removed from the data set. Run number simply refers to the experiment number from which each data point came.

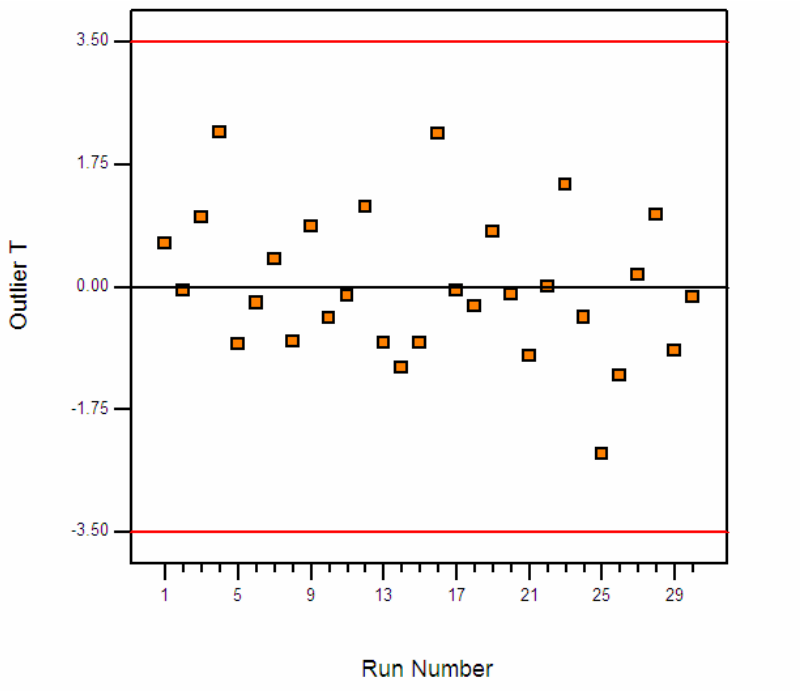

Figure 3.6 – Outlier T Values for Experimental Data Set

The experimental data set was also examined to determine if any points had a relatively larger influence on the model than others. Both leverage and Cook's distance functions were utilized for this analysis. Leverage assesses the influence of a single point on the model and Cook's distance measures how much the model would change if a specific point were removed. For the Fe(II) regeneration data, neither of these functions highlighted any real problem points.

Last, a plot of the actual vs. predicted values was generated, allowing visualization of how well the model predicts the experimental response (Figure 3.7). The values shown are the natural log of the actual and predicted Fe(II) regeneration rate.

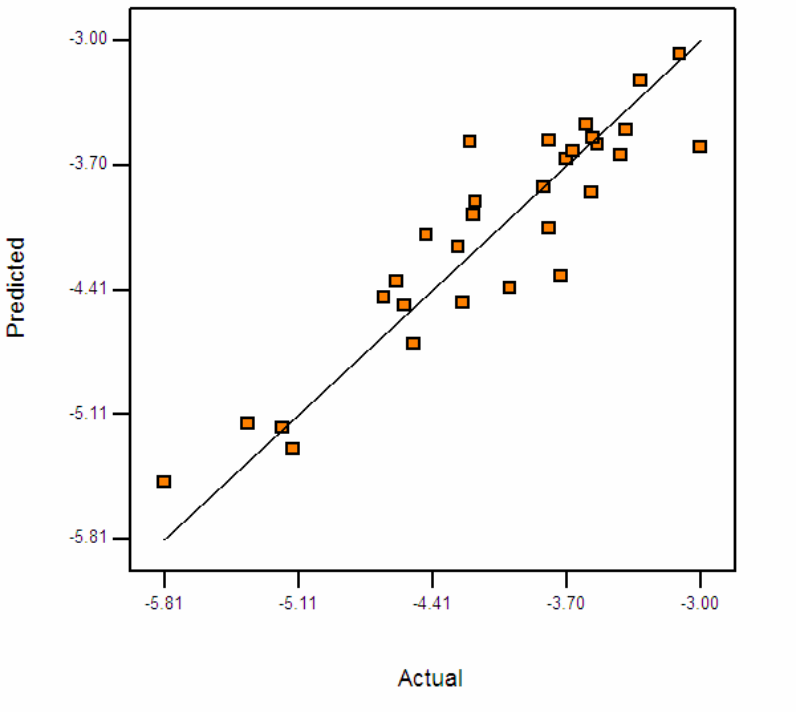

Figure 3.7 – Design Expert Model Predicted vs. Actual Values

As seen above, the correlation between the model and experimental data is very reasonable with the natural log transformation. The model predicts all points within 20% of the actual values, with only three points predicted to be more than 10% from the actual value.

With respect to the actual model expression, all process factors were included; however, only initial Fe(III) concentration and carbon particle size were included as linear terms. Initial SO_2 concentration and temperature were included as squared or two factor interaction (2FI) terms. A 2FI was also significant between the Fe(III) concentration and carbon size. The model expression is as follows in Equation 8, where $C_{Fe^{3+}}$ and C_{SO_2} are the initial Fe(III) and SO_2 concentrations, respectively, T is the reaction temperature, and S is the mean carbon particle size.

$$R_{model} = -3.64 + [0.47C_{Fe^{3+}}] - [0.54S] - [1.24T^2] - [0.27C_{SO_2} \times T] + [0.33C_{Fe^{3+}} \times S] \qquad (8)$$

The model coefficients are given in terms of coded factor values between -1 and 1, which correspond to the highest and lowest tested values of a factor. For example, coded values for the mean carbon particle size are -1, 0 and 1, which correspond to 499 μm, 649 μm and 843 μm, respectively.

The linear effects of both carbon particle size and initial Fe(III) concentration, and the relatively small influence of initial SO_2 concentration, are not surprising. As mentioned previously, since the carbon catalyzes the Fe(II) regeneration via the provision of surface area on which the reactants can adsorb and then react, a larger surface area promotes greater adsorption and, hence, faster reaction. Separate studies or the regeneration reaction kinetics show that the reaction is mass transfer-controlled by Fe(III) because the diffusivity of Fe(III) is much smaller than that of $SO_{2(aq)}$. This mechanism is confirmed by the significant model terms (Equation 8), including the 2FI between carbon particle size and Fe(III) concentration. This term can be logically explained considering that changes in carbon size will significantly affect the reaction rate by changing adsorption Fe(III), the rate limiting reactant.

Additionally, the highest reaction rates were observed during experiments at a temperature of about 120°F, with moderate SO_2 concentrations. This phenomenon is captured by the squared temperature term in the model expression (Equation 8); at a moderate temperature, the negative effect of the squared temperature term is minimized such that the Fe(II) regeneration rate is increased.

The fact that reaction temperature was not found to have a linear influence on the Fe(II) regeneration rate is rather surprising. Generally, increased temperature increases a chemical reaction rate, as well as diffusivity. However, the experimental data suggests that temperature alone does not significantly affect the reaction rate, but that the combination of temperature and initial SO_2 concentration do; this is confirmed by the 2FI model term that pairs the two quantities. At low SO_2 concentrations, increased reaction rate tended to correspond with increased temperature, as expected; however, at higher SO_2 concentrations, reaction rate decreased with increased temperature. These unpredicted results cannot be conclusively rationalized given the amount of data collected, but the dependence of reactant diffusivities on temperature might provide some explanation. At high temperature the SO_2 might reach the catalyst surface so much faster than the Fe^{3+} that it could inhibit Fe^{3+} adsorption, and hence the reaction. It seems that this would only become problematic if carbon surface area was low, but the temperature trends with SO_2 concentration did not

appear to differ much between the largest and smallest carbon particle sizes tested. Another explanation might focus on the solubility of SO_2, since as temperature increases, SO_2 solubility decreases; if air space was present at the top of the regeneration reactor, SO_2 may have collected there, reducing the concentration available for the reaction.

Given the relatively small significance of the 2FI term combining temperature and SO_2 concentration, indicated by its small coefficient in Equation 8, it may actually be removed from the model expression without substantially affecting the model fit for the ranges of factors tested. The other term coefficients are only changed slightly and the reduced model expression then becomes Equation 9.

$$R_{model} = -3.64 + [0.47C_{Fe^{3+}}] - [0.53S] - [1.25T^2] + [0.33C_{Fe^{3+}} \times S] \qquad (9)$$

Optimization

The Design Expert software offers three methods of optimization: point prediction, graphical and numerical. The numerical method determines the optimal combination(s) of process factors for user defined goals (i.e., desired responses), and generates a set of 10 solutions, which are ranked by desirability. This method was chosen for optimizing the Fe(II) regeneration since the stated goal of the problem was to maximize $R_{Fe^{2+}}$, thereby maximizing the regeneration rate without allowing break-through SO_2 in the reactor effluent. The most significant model expression (Equation 8) was used for optimization. The model was constrained to the boundaries of the design space for optimization such that it could not find solutions by extrapolating process factor values outside of their tested ranges.

At first, optimization was completed with the carbon particle size being allowed to fluctuate as a numeric factor (i.e., the model was not required to find a solution with the particle size being one of the discreet mean sizes tested). Although this is not practical because activated carbon is typically sold in established, discreet mesh sizes, allowing the particle size to fluctuate continuously showed whether a particular size was overwhelmingly desirable. Table 3.3 gives the 10 most desirable solutions for the combinations of process factors that maximize $R_{Fe^{2+}}$.

Table 3.3 – Optimization Solutions with Carbon Particle Size as a Numeric Factor

Solution #	Process Factors: Initial SO_2 Concentration (g/L)	Initial Fe(III) Concentration (g/L)	Reaction Temperature (°F)	Mean Carbon Particle Size (μm)	R_{model} (mol/L-min)	$R_{Fe^{2+}}$ (mol/L-min)	Desirability
1	0.78	5.97	121	506	-3.000	0.0498	1
2	0.76	5.90	120	509	-2.996	0.0500	1
3	0.82	5.95	120	499	-3.000	0.0498	1
4	0.72	5.94	122	499	-2.999	0.0498	1
5	0.71	5.92	121	512	-3.000	0.0498	1
6	0.75	5.99	121	519	-2.995	0.0501	1
7	0.71	5.90	120	499	-2.988	0.0504	1
8	0.74	5.98	119	507	-2.985	0.0505	1
9	0.81	5.99	120	505	-2.999	0.0498	1
10	0.78	3.09	120	499	-3.176	0.0418	0.94

The solutions in Table 3.3 confirm the expectation that the smallest carbon particle size (20x50 mesh, mean size 499 μm) is the optimal size of those tested. It provides much more surface area on which the Fe(II) regeneration reaction can occur, and probably a smaller size would allow an even faster reaction. The numerical optimization was completed again with the mean carbon particle size specified as 499 μm. Table 3.4 shows the 10 most desirable solutions.

Table 3.4 – Optimization Solutions with Carbon Particle Size Fixed at 499 μm

Solution #	Process Factors: Initial SO_2 Concentration (g/L)	Initial Fe(III) Concentration (g/L)	Reaction Temperature (°F)	Mean Carbon Particle Size (μm)	R_{model} (mol/L-min)	$R_{Fe^{2+}}$ (mol/L-min)	Desirability
1	0.81	6.00	120	499	-2.990	0.0503	1
2	0.75	5.96	122	499	-2.992	0.0502	1
3	0.78	5.99	120	499	-2.976	0.0510	1
4	0.71	5.99	120	499	-2.980	0.0508	1
5	0.75	5.81	120	499	-2.995	0.0501	1
6	0.78	5.97	118	499	-2.997	0.0499	1
7	0.72	6.00	121	499	-2.974	0.0511	1
8	0.75	5.98	121	499	-2.985	0.0506	1
9	0.77	5.81	120	499	-2.996	0.0500	1
10	0.78	2.00	120	499	-3.171	0.0420	0.94

Initial Fe(III) concentration is one of the two most influential model factors, the other being the carbon particle size. Since the reaction rate is controlled by the transport of Fe(III) to the carbon surface, it is reasonable that the highest Fe(III) concentration is the optimal value for maximizing the reaction rate. Likewise, the initial SO_2 concentration and temperature optimal values, which are both in the middle of the ranges tested, seem appropriate since the values are close to those used in experiments where the highest reaction rates were observed.

To actually optimize the Fe(II) regeneration process for a larger scale operation, reactor size and flow rate will require consideration. For a desired amount of Fe(II) regeneration, given the $R_{Fe^{2+}}$ value predicted by the model for any combination (within the design space) of the process factors, the reactor residence time can be determined (Equation 6). From the residence time, the reactor volume and flow rate can then be determined (Equation 5). It should be noted that, while many possible combinations of volumes and flow rates could be utilized to achieve a desired residence time, large changes to the flow rate may invalidate the model due to changes in reaction kinetics (i.e., the reactor flow rate can affect how easily reactants adsorb onto the carbon surface). This issue was not specifically addressed during the test-work for this optimization problem, but it was in a separate study, which is presented in Chapter 2.

Conclusions and Recommendations

The Fe(II) regeneration process is an important aspect of AART using FFS for copper hydrometallurgy; however little has been done to study it specifically. SO_2 has been chosen as the most attractive reducing agent for use in the process and, because the homogenous reaction between Fe(III) and SO_2 in solution is very slow, activated carbon is utilized as a surface catalyst. Although several factors may affect the regeneration reaction, few may be varied due to the place of the reaction within the scheme of the entire hydrometallurgical process. It is important to understand how those that are variable may be manipulated to produce desirable responses, for the purposes of process design and improvement. As such, the goals of this work were to examine and optimize a set of four variable factors: carbon particle size (i.e., surface area), temperature, and the initial concentrations of the reactants, Fe(III) and SO_2.

The most desirable response was defined as the maximum rate of Fe(II) regeneration at which there is no break-through SO_2 in the process effluent. Experiments were conducted to capture the effects of each factor on the regeneration rate. The experimental data were analyzed and modeled using Design Expert software. Finally, the model was optimized to determine a factor combination which resulted in the most desirable response.

The following conclusions can be made with respect to the major observations during experimentation, analysis and modeling:

- Break-through SO_2 in the process effluent increases exponentially with increased flow rate.
- The two-part experimental procedure appears to be capable of producing precise results, although there is likely some constant error associated with each experiment due to the inability to avoid air space at the top of the reactor.
- Data analysis and modeling using Design Expert software proved successful methods for relating multiple factors to a response for the Fe(II) regeneration process.
- The generated model is statistically significant, and predicts all experimental data points within 20% of their values.
- Carbon particle size and initial Fe(III) concentration are the most influential process factors and are included as linear terms in the model.
- Temperature is also significant and included as a squared term in the model, which results in an optimal temperature within the range of tested values.
- Initial SO_2 and temperature are not linearly influential; however, the combination of the two factors was determined to slightly affect the Fe(II) regeneration rate, but the effect cannot be conclusively explained.

Using the software-generated model to optimize the Fe(II) regeneration process within the tested variable ranges, it was confirmed that the smallest carbon particle size in combination with the highest initial Fe(III) concentration generally produces the fastest regeneration rates. Additionally, by operating the process with temperature and initial SO_2 concentration at moderate values, the regeneration rate is maximized.

Furthermore, several recommendations can be made regarding additional test-work and scale-up operations for the Fe(II) regeneration. First, the results of the current work might be used as the design basis for future experiments. The most influential factors may be tested within a wider range of values, and some conclusions made with respect to the economy of changing operating parameters to improve process results. A better understanding of the

effects of temperature and initial SO_2 concentration might also be gained from experimenting over a wider range of values. Next, some tests to determine the lifetime of the activated carbon may be necessary. Issues including deactivation and wear (e.g., abrasion by electrolyte flow and between carbon particles) are likely to be important in estimating how often carbon may need to be replaced. Finally, several observations from the current work may be useful in designing large-scale operations, including those regarding break-through SO_2 and flow rate trends, and problems associated with air space at the top of the regeneration reactor. Such observations, combined with the results from the optimization problem, would be useful in making general decisions as to the safest, most efficient operating parameters.

Chapter 4: Summary, Conclusions and Recommendations

Summary

Copper is essential to modern society and demand for the commodity will continue to grow with global populations and economies (Demler, 2005). Due to its unique properties, the metal has an array of end uses, most importantly as an electrical conductor and a corrosion-resistant construction material. A major method of processing mined copper ore is hydrometallurgy, which utilizes the electrical properties of copper to finally extract the pure metal during a process called electrowinning (EW). EW accounts for a large percentage of the total processing costs for hydrometallurgy, as it has substantial power requirements. In an effort to reduce the power consumption by copper EW operations, Alternate Anode Reaction Technology (AART) is being investigated. This technology is attractive because of its considerably lower energy requirement and added benefits, namely elimination of acid misting in EW tank-houses and by-production of recoverable acid. A major aspect of AART is regeneration of the anode reactant, Fe(II), which is achieved by reducing Fe(III) with SO_2. The Fe(III)-SO_2 reaction is catalyzed by activated carbon particles, since the homogenous reaction is slow in aqueous solution (Sandoval and Dolinar, 1996).

Until now, little has been done to specifically the study the Fe(II) regeneration process, however a better understanding may provide insight into improvement of the current process and/or associated materials or equipment. Given its place within the scheme of the EW circuit, and the overall hydrometallurgical process, many Fe(II) regeneration process parameters are fixed or have limited variability. Fixed conditions, including acid and sulfate concentrations, are relatively extreme, making comparison to other studied processes difficult. While the regeneration process has been successfully operated at both the bench and pilot scale, variable factors, like reactant concentrations and carbon particle size, have not been examined to determine their effects. Additionally, the mechanism of Fe(III)-SO_2 reaction in the presence of the carbon catalyst has not been verified.

To gain a better understanding of the Fe(II) regeneration and improve process results, two studies were conducted and the details are presented in this work. The first study surrounded the fundamental kinetics of the Fe(II) regeneration reaction with the purpose of developing and validating a rate model. The purpose of the second study was to determine the basic effects several variable factors, and then optimize the regeneration process by finding a combination of the factors which produced the most desirable results.

Conclusions

The study surrounding the fundamental kinetics of the Fe(II) regeneration resulted in validation of the hypothesized mass transfer model shown below in Equation 1:

$$\frac{dFe^{2+}}{dt} = \frac{6M}{\rho dV}\left[\frac{2D_f}{d} + 0.6\frac{V_t^{1/2} D_f^{2/3}}{d^{1/2} v^{1/6}}\right][C_{Fe^{3+}}]^x \qquad (1)$$

which predicts the rate of Fe(II) regeneration, $\frac{dFe^{2+}}{dt}$ (mol/L-min), under the tested conditions. M (g) is the mass of the carbon, d (cm) is the mean diameter of carbon particles, V (mL) is the volume of the solution within the carbon bed, p (g/cm3) is the carbon density, D_f (cm^2/min) is the diffusion coefficient of Fe(III), V_t (cm/min) is the slip velocity of the solution, v (cm^2/min) is the kinematic viscosity of the solution, and $C_{Fe^{3+}}$ (g/mL) is the initial Fe(III) concentration. The observed D_f was 1.1×10^{-7} cm^2/s (6.6×10^{-6} cm^2/min). Additionally, the following conclusions were made about the Fe(II) regeneration reaction:

- Because it accounts for the reaction mechanism, a mass transfer rate model predicts the Fe(II) regeneration rate more accurately and precisely than a general model.
- The reaction rate is first-order (i.e., x = 1 in the above model equation), and is limited by the rate at which Fe(III) diffuses onto the carbon particle surfaces.
- Initial concentration of $SO_{2(aq)}$ does not significantly affect the reaction rate.
- The reaction rate is significantly increased by increased initial Fe(III) concentration or decreased carbon particle size.
- Flow rate significantly affects the diffusivity of a species; as a result, reaction rate is inhibited at very high flow rates.

The optimization study also has an associated model to predict Fe(II) regeneration rate, which was generated by analyzing data from a series of experiments within a defined design space. The regeneration rate investigated during this study was constrained; it was considered the fastest rate at which there was no or negligible SO_2 in the process effluent. Experimental design, data analysis, modeling and optimization were completed using Design Expert software by Stat-Ease. Under the tested conditions – varied ranges of carbon particle size, temperature and initial Fe(III) and SO_2 concentrations – the model response is a function of all four factors. The model is given by the following (Equation 2):

$$R_{model} = \ln(R_{Fe^{2+}}) = -3.64 + [0.47C_{Fe^{3+}}] - [0.54S] - [1.24T^2] - [0.27C_{SO_2} \times T] + [0.33C_{Fe^{3+}} \times S] \quad (2)$$

which actually predicts the natural logarithm of the Fe(II) regeneration rate, $R_{Fe^{2+}}$. S is carbon particle size, T is temperature, and $C_{Fe^{3+}}$ and C_{SO_2} are the initial concentrations of Fe(III) and SO_2, respectively. Equation 2 is given in terms of coded factor values between -1 and 1, which correspond to the highest and lowest tested values of a factor. It has only been verified within the tested ranges of each factor.

The following conclusions were made regarding the major observations, data analysis and the generated model:

- Break-through SO_2 in the process effluent increases exponentially with increased flow rate.
- The two-part experimental procedure appears to be capable of producing precise results, although there is likely some constant error associated with each experiment due to the inability to avoid air space at the top of the reactor.
- Data analysis and modeling using Design Expert software proved successful methods for relating multiple factors to a response for the Fe(II) regeneration process.
- The generated model is statistically significant, and predicts all experimental data points within 20% of their values.
- Carbon particle size and initial Fe(III) concentration are the most influential process factors and are included as linear terms in the model.
- Temperature is also significant and included as a squared term in the model, which results in an optimal temperature within the range of tested values.

- Initial SO_2 and temperature are not linearly influential; however, the combination of the two factors was determined to slightly affect the Fe(II) regeneration rate, but the effect cannot be conclusively explained.

Upon optimization of the model (Equation 2) to maximize $R_{Fe^{2+}}$, the following combination of process factors was determined optimal: maximum initial Fe(III) concentration, minimum carbon particle size, and moderate values of temperature and initial SO_2 concentration.

The findings of both studies coincide well with each other. Each determined that carbon particle size and initial Fe(III) concentration were the most influential factors for the Fe(II) regeneration process. Also, the initial SO_2 concentration was determined to be of least significance to the reaction rate. The reaction mechanism – reactant adsorption and subsequent reaction on the carbon surface – was confirmed by the kinetics study and supported by the results of the optimization study. While the results of each study are only known to be applicable under the tested conditions, they provide some insight into Fe(II) regeneration in larger scale processes. Through a better understanding of the regeneration process, commercial processes may be better designed or improved.

Recommendations

Following is a list of topics surrounding the Fe(II) regeneration process for AART using FFS that may require further work:

- determination and quantification of the effects of reaction temperature on the process responses;
- quantification of the effects of solution flow rate through the regeneration reactor on reactant diffusivities, and, hence, process responses;
- determination of the effects of carbon type on the process responses;
- determination of factors contributing to carbon deactivation, and quantification of carbon lifetime; and,
- validation of the Fe(II) regeneration rate models outside of the factor ranges tested in this work.

References

1. International Copper Study Group (ICGS), *2003 Copper Bulletin*. Vol. 10, No. 1, Lisbon, Portugal, January 2003.
2. London Metal Exchange (LME), <http://www.lme.co.uk/dataprices_daily_metal.asp>. Updated daily, accessed June 2005.
3. Demler, F., *Copper Outlook* <http://www.manmetals.com/research/copper022005.pdf>. Man Financial, Ltd., member of LME, February 2005.
4. Dresher, W., *Copper Applications in Mining and Metallurgy*, <http://www.copper.org/innovations/2001/08/hydrometallurgy.html>, August, 2001, accessed May 2005.
5. Dolinar, W. J., and S. P. Sandoval, *Copper Electrowinning in the Absence of Acid Misting Using the Ferrous/Ferric-Sulfur Dioxide Anode Reaction – A Pilot Study*. Transactions of Society for Mining, Metallurgy, and Exploration, Inc., Vol. 298, pp. 1936-42, 1996.
6. Sandoval, S. P., and K. P. V. Lei, *Evaluation of the Ferrous/Ferric-Sulfur Dioxide Anode Reaction for Integration into the Copper Leaching-Solvent Extraction-Electrowinning Circuit*. Proceedings of Milton E. Wadsworth (IV) International Symposium on Hydrometallurgy, Salt Lake City, UT, pp. 1091-1105, August 1-5, 1993.
7. Sandoval, S. P., W. J. Dolinar, J. W. Langhans Jr., and K. P. V. Lei, *A Substituted Anode Reaction for Electrowinning Copper*. Proceedings of Copper 95 International Conference, Santiago, Chile, November 26-29, 1995.
8. Shriver, D. and P. Atkins, Inorganic Chemistry. 3rd edition, W. H. Freeman and Company, New York, NY, 2003.
9. Kumar, S., V. M. H. Govindarao, and M. Chanda, *Oxidation of aqueous sulfur dioxide catalyzed by poly-4-vinylpyridine-Cu(II) complex; Part 1: homogeneous phase oxidation*. J. Chem. Tech. BioTech, Vol. 67, pp. 39-52, 1996.
10. Govindarao, V. M. H. and K. V. Gopalakrishna, *Oxidation of sulfur dioxide in aqueous suspensions of activated carbon*. Ind. Eng. Chem. Res., Vol. 34, pp. 2258-71, 1995

11. García, E., G. R. Dieckmann, and S. H. Langer, *Electrogenerative formation of ferric ions in a sulfur dioxide–sulfuric acid solution; Graphite catalysed sulfur dioxide oxidation.* Journal of Applied Electrochemistry, Vol. 28, Issue 10, pp. 1127-36, October 1998.
12. Thomas, G., and T. R. Ingraham, *Kinetics of the Carbon Catalyzed Air Oxidation of Ferrous Ion in Sulphuric Acid Solutions*. Unit Processes in Hydrometallurgy, Vol. 24, pp. 67-79, 1963.
13. Seaburn, J. T. and A. J. Engel, *Sorption of sulfur dioxide by suspension of activated carbon in water*. AIChE J., Vol. 134, pp. 71-5, 1993.
14. Komiyama, H. and J. M. Smith, *Sulfur dioxide oxidation in slurries of activated carbon: Part I-Kinetics*. AIChE Journal, Vol. 21, pp. 664-70, 1975.
15. Krissman, J., M. Siddiqi, and K. Lucas, *Thermodynamics of SO_2 Absorption in Aqueous Solutions*. Chem. Eng. Technology, Vol. 8, 1998.
16. Berglund, J., S. Fronaeus, and L. I. Elding, *Kinetics and mechanism for manganese-catalyzed oxidation of sulfur(IV) by oxygen in aqueous solution*. Inorg. Chem., Vol 32(21), pp. 4527-4538, 1993.
17. Han, K., *The Effect of Concentration and Temperature on Diffusivity of Metal Compounds*. Metallurgical Transactions B, Vol. 21B, pp. 429-438, June, 1990.
18. Freiberg, J. E., and S. E. Schwartz, *Oxidation of SO_2 in Aqueous Droplets: Mass-Transport Limitation in Laboratory Studies and the Ambient Atmosphere. Atmospheric Environment*. Vol. 15, No. 7, pp. 1145-1154, 1981.
19. Ramsing, N. and J. Gundersen, *Seawater and Gases: Tabulated Physical Parameters of Interest to People Working with Microsensors in Marine Systems*. Unisense, Denmark.
20. Cook, P., "*SO_2 Measurement.*" Email to Emily A. Sarver, November 4, 2004.
21. Occupational Safety and Health Administration (OSHA), Chemical Sampling Information: Sulfur Dioxide, <http://www.osha.gov/dts/chemicalsampling/data/CH_268500.html>. Updated June 2005, accessed June 2005.
22. Wood, W. G., ed., ASM Handbook: Volume 5, Surface Engineering. American Society for Metals, Metals Park, OH, 1994.

23. Whan, R. E., ed., ASM Handbook: Volume 10, Materials Characterization. American Society for Metals, Metals Park, OH, 1992.
24. Han, K., Aqueous Metallurgy. Society for Mining, Metallurgy and Exploration, Littleton, CO, Vol. 1, 2002.
25. Anderson, M., ed. Design Expert User's Guide. Stat-Ease, Inc. 2002.
26. Jergensen II, G., ed. Copper Leaching, Solvent Extraction and Electrowinning. Society for Mining, Metallurgy and Exploration, Littleton, CO, 1999.

Appendix A

Table A.1 – Complete Summary of Experimental Data

Experiment	Mean Carbon Particle Size	Carbon Density	Flow rate	Initial Fe(III) Concentration		Initial SO_2 Concentration		$\frac{dFe^{2+}}{dt}$ observed
#	μm	g/cm^3	mL/min	g/L	mol/L	g/L	mol/L	mol/L-min
a1	843	1.24	80	0.60	0.011	3.00	0.047	0.0039
a2	843	1.24	80	0.60	0.011	3.00	0.047	0.0041
a3	843	1.24	125	0.90	0.016	0.75	0.012	0.0120
a4	843	1.24	125	1.90	0.034	0.75	0.012	0.0124
a5	843	1.24	125	1.90	0.034	1.00	0.016	0.0212
a6	843	1.24	125	2.70	0.048	0.31	0.005	0.0094
a7	843	1.24	125	2.70	0.048	0.50	0.008	0.0127
a8	843	1.24	125	2.70	0.048	0.75	0.012	0.0118
a9	843	1.24	168	3.34	0.060	0.75	0.012	0.0183
a10	843	1.24	125	3.90	0.070	0.75	0.012	0.0162
a11	843	1.24	230	4.07	0.073	1.00	0.016	0.0246
a12	843	1.24	110	4.47	0.080	2.00	0.031	0.0171
a13	843	1.24	125	4.47	0.080	1.25	0.020	0.0170
a14	843	1.24	175	4.47	0.080	1.25	0.020	0.0131
a15	843	1.24	175	4.47	0.080	0.75	0.012	0.0119
a16	843	1.24	125	5.45	0.098	1.25	0.020	0.0220
a17	843	1.24	110	5.45	0.098	2.00	0.031	0.0285
a18	843	1.24	175	5.57	0.100	0.75	0.012	0.0277
a19	843	1.24	125	5.90	0.106	0.75	0.012	0.0147
a20	843	1.24	125	7.21	0.129	1.25	0.020	0.0269
a21	843	1.24	175	7.73	0.138	0.75	0.012	0.0297
a22	843	1.24	175	9.59	0.172	1.25	0.020	0.0326
a23	843	1.24	110	9.59	0.172	2.00	0.031	0.0260
a24	843	1.24	125	9.59	0.172	1.25	0.020	0.0321
a25	843	1.24	350	12.83	0.230	0.60	0.009	0.0383
a26	843	1.24	390	12.85	0.230	0.57	0.009	0.0352
a27	843	1.24	320	12.90	0.231	0.75	0.012	0.0415
b1	649	1.26	188	1.42	0.025	0.75	0.012	0.0225
b2	649	1.26	220	3.88	0.069	0.75	0.012	0.0328
b3	649	1.26	230	4.06	0.073	1.00	0.016	0.0314
b4	649	1.26	214	4.24	0.076	0.75	0.012	0.0283
b5	649	1.26	215	4.50	0.081	1.00	0.016	0.0273
b6	649	1.26	240	4.50	0.081	0.75	0.012	0.0337
b7	649	1.26	292	4.57	0.082	0.50	0.008	0.0290
b8	649	1.26	261	6.03	0.108	0.75	0.012	0.0364
c1	499	1.33	194	2.46	0.044	1.00	0.016	0.0246
c2	499	1.33	230	4.07	0.073	1.00	0.016	0.0351
c3	499	1.33	272	4.48	0.080	0.75	0.012	0.0497
c4	499	1.33	270	4.51	0.081	0.75	0.012	0.0446

Table A.2 – Complete Summary of Experimental vs. Modeled Fe(II) Regeneration Rate

Experiment	Flow rate	Initial Fe(III) Concentration	Initial SO2 Concentration	$\frac{dFe^{2+}}{dt}$ observed	General Model $\frac{dFe^{2+}}{dt} = k'[C_{Fe^{3+}}]^1$	Error	Mass Transfer Model $\frac{dFe^{2+}}{dt} = \frac{6M}{\rho d V}\left[\frac{2(1.1\times10^{-7})}{d} + 0.6\frac{V_t^{1/2}(1.1\times10^{-7})^{2/3}}{d^{1/2}\nu^{1/6}}\right][C_{Fe^{3+}}]^1$	Error
#	mL/min	g/L	g/L	mol/L-min	mol/L-min	%	mol/L-min	%
a1	80	0.60	3.00	0.0039	0.0020	-48.1	0.0017	-56.2
a2	80	0.60	3.00	0.0041	0.0020	-50.8	0.0017	-58.5
a3	125	0.90	0.75	0.0120	0.0031	-74.5	0.0032	-73.4
a4	125	1.90	0.75	0.0124	0.0065	-48.0	0.0067	-45.7
a5	125	1.90	1.00	0.0212	0.0065	-69.5	0.0067	-68.1
a6	125	2.70	0.31	0.0094	0.0092	-2.9	0.0096	1.5
a7	125	2.70	0.50	0.0127	0.0092	-27.5	0.0096	-24.3
a8	125	2.70	0.75	0.0118	0.0092	-22.3	0.0096	-18.8
a9	168	3.34	0.75	0.0183	0.0114	-38.0	0.0137	-25.2
a10	125	3.90	0.75	0.0162	0.0132	-18.3	0.0138	-14.6
a11	230	4.07	1.00	0.0246	0.0138	-43.8	0.0194	-21.1
a12	110	4.47	2.00	0.0171	0.0152	-11.3	0.0149	-12.8
a13	125	4.47	1.25	0.0170	0.0152	-10.7	0.0159	-6.6
a14	175	4.47	1.25	0.0131	0.0152	16.0	0.0187	42.6
a15	175	4.47	0.75	0.0119	0.0152	27.6	0.0187	56.9
a16	125	5.45	1.25	0.0220	0.0185	-15.9	0.0193	-12.1
a17	110	5.45	2.00	0.0285	0.0185	-35.2	0.0182	-36.3
a18	175	5.57	0.75	0.0277	0.0189	-31.7	0.0233	-16.0
a19	125	5.90	0.75	0.0147	0.0200	36.0	0.0209	42.2
a20	125	7.21	1.25	0.0269	0.0245	-8.9	0.0256	-4.7
a21	175	7.73	0.75	0.0297	0.0263	-11.6	0.0323	8.8
a22	175	9.59	1.25	0.0326	0.0326	-0.1	0.0400	22.9
a23	110	9.59	2.00	0.0260	0.0326	25.2	0.0320	23.1
a24	125	9.59	1.25	0.0321	0.0326	1.6	0.0340	6.2
a25	350	12.83	0.60	0.0383	0.0436	13.6	0.2009	423.9
a26	390	12.85	0.57	0.0352	0.0436	23.9	0.2013	471.6
a27	320	12.90	0.75	0.0415	0.0438	5.7	0.2023	387.8
b1	188	1.42	0.75	0.0225	0.0098	-56.3	0.0089	-60.4
b2	220	3.88	0.75	0.0328	0.0268	-18.1	0.0263	-19.9
b3	230	4.06	1.00	0.0314	0.0281	-10.5	0.0281	-10.5
b4	214	4.24	0.75	0.0283	0.0294	3.8	0.0283	0.2
b5	215	4.50	1.00	0.0273	0.0311	14.1	0.0301	10.4
b6	240	4.50	0.75	0.0337	0.0311	-7.7	0.0318	-5.9
b7	292	4.57	0.50	0.0290	0.0316	9.1	0.0355	22.4
b8	261	6.03	0.75	0.0364	0.0417	14.6	0.0443	21.8
c1	194	2.46	1.00	0.0246	0.0244	-0.6	0.0224	-8.9
c2	230	4.07	1.00	0.0351	0.0405	15.4	0.0403	14.9
c3	272	4.48	0.75	0.0497	0.0446	-10.3	0.0482	-3.2
c4	270	4.51	0.75	0.0446	0.0449	0.7	0.0483	8.3

Appendix B

Part 1: Orders of Reaction

To confirm that SO_2 concentration is not significant to the Fe(II) regeneration rate under the tested conditions, a plot was generated to look at the relative change in reaction rates with particle size and initial reactant concentrations. The regeneration rate was plotted separately for each particle size as a function of the product of first-order initial Fe(III) and SO_2 concentrations. A total of six points were removed from the data set due to suspected errors either in experimentation (e.g., excessive SO_2 escape from the reactor) or in assay analyses (i.e., the measured Fe(II) product was higher than theoretically possible). The resulting plot (Figure B.1) shows the trend of the data for each tested carbon size; the solid lines represent linear trend-lines for the regeneration rate for each carbon size, and the points represent the experimental data.

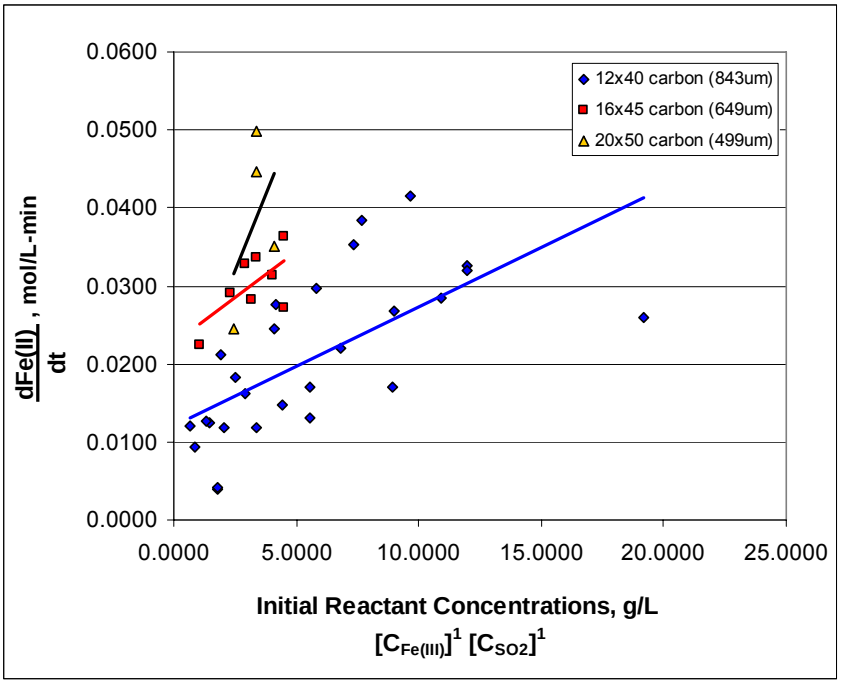

Figure B.1 – Fe(II) Regeneration Rate as a Function of First-Order Initial Fe(III) and SO_2 Concentrations

Looking back to Equation 10, when the orders of the reactants, *x* and *y*, are equal (i.e., Fe(III) and SO_2 are considered to have the same degree of influence on the reaction rate) the rate constant, *k*, is the slope of the solid line in Figure B.1 for each carbon size. From the

wide scatter in the data in Figure B.1 it is clear that the reactants do not have equal orders, so a function was created to solve for the values of k, x and y that minimize the squared difference between the actual data points and the rate calculated by Equation 10 for each carbon size. The resulting values are given in Table B.1.

Table B.1 – Solved Values of k, x and y

Carbon Size	k	x	y
Mesh	1/min	Fe(III) Concentration	Order of SO_2 Concentration
12x40	0.100	0.62	0.02
16x45	0.070	0.30	0.01
20x50	0.730	1.11	0.00

Because the order of $[C_{Fe^{3+}}]$ for each size class was overwhelmingly greater than that of $[C_{SO_2}]$, the stated expectation that Equation 10 could be reduced to Equation 12 was confirmed; therefore, $[C_{SO_2}]$ was assumed to have a constant order of zero (i.e., $y = 0$ and $[C_{SO_2}]^y = 1$), and only the initial concentration of Fe(III) required inclusion in the Fe(II) regeneration rate model for the ranges of conditions examined.

Part 2: Fe(III) Diffusivity

From the final hypothesized mass transfer model (Equation 17), it is clear that Fe(III) diffusion, kinematic viscosity, and slip velocity are additional influences on the Fe(II) regeneration rate. Kinematic viscosity was calculated per Equation 15 and slip velocity per Equation 14. Diffusion was determined from the experimental data since the value was unknown for the process conditions tested.

By fitting D_f, the mass transfer model could be applied to the experimental data. An Excel solver function was used to fit D_f. With a first-order dependence on Fe(III) (i.e., $x = 1$), the corresponding D_f was calculated as 1.1×10^{-7} cm^2/s. These values give the model a very good fit to most of the data, the exceptions are explained below. Fe(II) regeneration rate values predicted by the mass transfer model are given in Appendix A (Table A.2) and compared to observed (experimental) values. Figure B.2 shows the model predicted rate

values plotted against the observed values over the entire tested range of initial Fe(III) concentration and flow rate; the solid line is a linear trend-line.

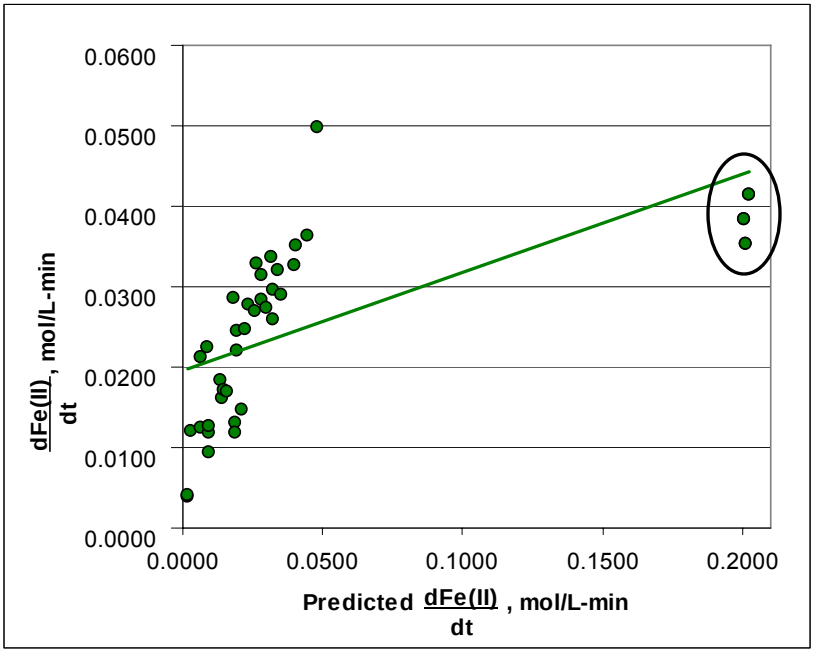

Figure B.2 – Experimental Fe(II) Regeneration Rate Values vs. Mass Transfer Model Over Entire Initial Fe(III) Concentration and Flow Rate Ranges

The three circled points in Figure B.2 clearly throw off the trend of the experimental vs. predicted rate values, which are associated with three of the experiments utilizing the 12x40 mesh carbon. The model severely over-estimates the Fe(II) regeneration for these points, which represent experiments with both very high initial Fe(III) to SO_2 ratios and flow rates. These conditions may explain the over-estimation of the model as follows. Due to the relatively large Fe(III) to SO_2 ratio used in generating these points, all of the SO_2 may have been consumed in a shorter time than the tested residence time for these experiments. With respect to the high flow rates, they were applied in an effort to determine the reaction rate, since at low flow rates the reaction would have definitely been completed faster than allowed by the residence time. However, extreme flows may have negatively affected Fe(III) diffusivity. It seems logical that as the flow rate is dramatically increased, turbidity and shear speed of electrolyte flowing past the carbon will inhibit Fe(III) adsorption.

Although not to the extent of the circled points in Figure B.2, the model under-estimates the Fe(II) regeneration rate for experiments with the lowest Fe(III) concentrations

and flow rates tested. Similar effects as proposed above might also explain the poor correlation between the model and experimental data at the low end of the initial Fe(III) concentration and flow rate ranges. It is possible that the reaction may have neared completion (i.e., most Fe(III) was consumed) faster than allowed by the tested residence times. As well, at very low flow rates, Fe(III) diffusivity may be increased and result in higher Fe(II) regeneration rates than those predicted by the mass transfer model. While more data would be necessary to conclusively explain this lack of fit between the model and experimental data discussed above, opposite trends at opposite ends of the tested Fe(III) concentrations and flow rate ranges support the offered explanations. Because the currently operable range of initial Fe(III) concentration and residence time (corresponding to tested flow rate) are well below those used to generate the circled points in Figure B.2, they can be removed from the data set without sacrificing the worth of the model for use in commercial design and operation of the Fe(II) regeneration process.

For the reduced data set, the average D_f value of 1.1×10^{-7} cm^2/s makes the mass transfer model fit the data well. This value is much lower than that found in the literature, 3.5×10^{-6} cm^2/s (Han, 1990). While the solute (sulfate) concentration for the current work and the study in the literature are similar, other conditions are quite different. Particularly the continuously flowing nature of the process in the current work, as opposed to more batch-type experiments used to determine diffusivity in the literature, provides some explanation for the large spread in the calculated and published D_f values. The flow of electrolyte (containing reactants) past the carbon particles inhibits adsorption of both species onto the catalyst, thereby inhibiting reaction. Countering the reduced diffusivity, it is conceivable that turbid conditions might also encourage reaction somewhat by increasing collision of reactants, and perhaps even reactants and carbon particles near the top of the carbon bed; however, this effect would probably not be nearly as noticeable as decreased diffusivity. For the current Fe(II) regeneration operating parameters, including residence times (flow rates) and Fe(III) concentrations, the model appears to predict the regeneration rate fairly accurately; however, to model such a process under more extreme conditions, it may be necessary to include D_f as a function of flow rate.

Part 3: Model Fit for Each Tested Carbon Particle Size

In addition to evaluating the overall fit of the mass transfer model to the experimental data, it should also be evaluated for each tested carbon particle size. Figure B.3 shows the model predicted Fe(II) regeneration rate values plotted against the observed values. The data is separated by carbon particle size used to generate it.

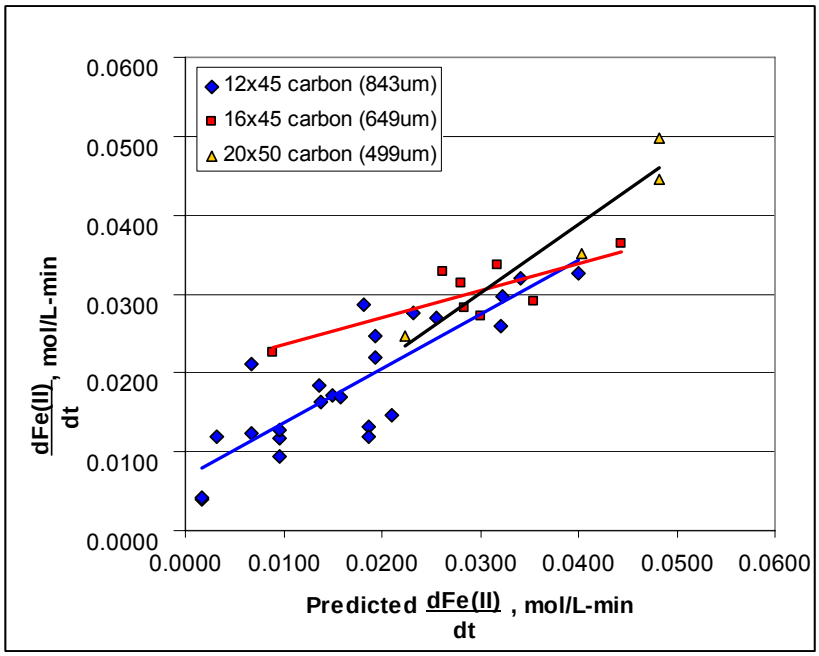

Figure B.3 – Experimental Fe(II) Regeneration Rate Values vs. Mass Transfer Model

The slope of the trend-lines for the large (12x40 mesh) and small (20x50 mesh) carbon sizes are still relatively close to one (0.70 and 0.90, respectively), indicating good model fit. Scatter in the 12x40 mesh data ($R^2 = 0.72$) is most likely due to difficulties during experimentation, including being able to ensure an airtight reactor and maintain a constant temperature. There are only a small number of data points for the 20x50 mesh carbon ($R^2 = 0.91$), so the model could be validated with more confidence for this carbon size with additional tests.

As for the 16x45 mesh carbon ($R^2 = 0.63$), the slope of the trend for the experimental vs. model values is flat (0.35), and it should be equal to one. From the data summary, the model under-estimates the Fe(II) regeneration rate at low initial Fe(III) concentration and over-estimates at high initial Fe(III) concentration. Since the model predicts too low at one

end and too high at the other, inclusion of the mid-sized carbon data does not significantly influence the overall mass transfer model (Figure 2.8); leaving out the data points only increases the slope of the plot from 0.75 to 0.78. Additionally, there does not appear to be significant influence by flow rate as was the case for more severe lack of fit issues seen in Figure 2.7. Since there are very few data points for this carbon size, one possibility for poor correlation is erroneous data, which could only be ruled out by conducting more tests. Another explanation may be attributable to the source of the carbon, which was crushed and screened during the current work since 16x45 mesh was not available from the carbon supplier for the experiments. Although care was taken to size the material accurately (e.g., using ASTM certified screens and mechanical shaker), the trend of the experimental data indicates that perhaps the carbon had a mean size larger than 649μm, the geometric mean size for 16x45 mesh particles. While it seems more likely that fines may bias an experiment with carbon sized by the user, it is possible that the size distribution was skewed toward the larger end of the mesh class. It may prove beneficial to test more carbon sizes which are all obtained from the same source; this will help eliminate errors caused by skewed size distributions and provide more data to further validate the kinetic model.

Appendix C

Table C.1 – Complete Summary of Experimental Data

Experiment #	Process Factors: Initial SO_2 Concentration (g/L)	Process Factors: Initial Fe(III) Concentration (g/L)	Process Factors: Reaction Temperature (°F)	Process Factors: Mean Carbon Particle Size (μm)	Process Responses: Flow Rate (mL/min)	Process Responses: Minimum Residence Time (min)	Process Responses: $R_{Fe^{2+}} = \frac{dFe^{2+}}{t_{min}}$ (mol/L-min)
1	0.50	4.6	116	649	292	0.523	0.0290
2	0.75	1.4	126	649	188	0.801	0.0225
3	0.75	4.5	111	649	186	0.821	0.0239
4	0.75	4.5	116	649	272	0.554	0.0497
5	0.75	4.5	119	649	214	0.704	0.0337
6	0.75	4.2	119	649	216	0.707	0.0224
7	0.75	3.9	118	649	220	0.676	0.0328
8	0.75	4.0	120	649	240	0.619	0.0148
9	0.75	4.2	124	649	240	0.619	0.0283
10	0.75	4.0	126	649	314	0.480	0.0118
11	0.75	6.0	121	649	261	0.585	0.0364
12	1.00	4.5	119	649	215	0.710	0.0273
13	0.50	2.6	113	843.5	129	1.178	0.0058
14	0.50	2.8	130	843.5	156	0.974	0.0055
15	0.50	6.2	112	843.5	169	0.899	0.0101
16	0.50	6.5	129	843.5	252	0.611	0.0281
17	0.75	3.3	122	843.5	168	0.917	0.0183
18	1.00	2.4	115	843.5	80	1.900	0.0046
19	1.00	2.0	128	843.5	106	1.434	0.0030
20	1.00	6.1	112	843.5	114	1.333	0.0151
21	1.00	6.4	130	843.5	172	0.895	0.0105
22	0.49	2.9	110	499	276	0.553	0.0094
23	0.50	2.5	134	499	326	0.468	0.0140
24	0.50	6.3	109	499	336	0.454	0.0143
25	0.50	5.2	131	499	326	0.468	0.0218
26	0.75	4.5	121	499	270	0.565	0.0446
27	1.00	2.5	112	499	194	0.787	0.0246
28	1.00	2.1	134	499	204	0.748	0.0110
29	0.98	6.2	111	499	248	0.615	0.0255
30	1.00	5.2	129	499	236	0.647	0.0153

Table C.2 – Comparison of Major Statistical Measurements for Central Composite and "Historical" Design Types for Experimental Data Set

Statistical Measure	Description*	Central Composite Design	"Historical" Design
G-Efficiency	calculated from the design points, this is the average prediction variance as a percentage of the maximum prediction variance. It is desirable to have an efficiency of at least 50%.	75.9%	64.1%
Condition Number in Correlation Matrix	this indicates the degree of multicollinearity present in the design matrix. If the value equals one, there is no multicollinearity and the design is orthogonal. If the value is less than 100 then there is not a serious problem. Values in the range of 100 to 1000 indicate moderate to severe multicollinearity and over 1000 indicates a severe problem.	11.4	14.8
Aliased Model Terms	these terms cannot be separated during analysis, due to too few data points	none	none
Large Variance Inflation Factors (VIF)	VIF measures how much the variance of a model coefficient increases due to the lack of orthogonality in the design. Specifically the standard error of a model coefficient increases in proportion to the square root of the VIF. If a coefficient is orthogonal to the remaining model terms, its VIF is one. One or more large VIFs indicate multicollinearity. VIFs exceeding ten indicate problems due to multicollinearity. (For example, if a coefficient has a VIF of 16, its standard error is 4 times as large as it would be in an orthogonal design.)	none	none

* Descriptions were obtained from the Design Expert 6 User's Guide (2002).

Table C.3 – Complete Design Evaluation by Design Expert Software

4 Factors: A, B, C, D

Design Matrix Evaluation for Response Surface Quadratic Model

No aliases found for Quadratic Model

Degrees of Freedom for Evaluation

Model	14.0000
Residuals	15.0000
Lack 0f F	15.0000
Pure Erro	0.0000
Corr Total	29.0000

				Power at 5 % alpha level for effect of		
Term	StdErr**	VIF	Ri-Squared	1/2 Std. Dev.	1 Std. Dev.	2 Std. Dev.
A	0.2498	1.115	0.103	15.5 %	46.6 %	96.2 %
B	0.2689	1.185	0.156	14.0 %	41.3 %	93.5 %
C	0.2806	1.277	0.217	13.3 %	38.5 %	91.4 %
D	0.2710	1.335	0.251	13.9 %	40.8 %	93.1 %
A2	0.6067	2.626	0.619	12.1 %	33.9 %	86.9 %
B2	0.4688	1.926	0.481	17.0 %	51.4 %	97.8 %
C2	0.7172	3.399	0.706	10.0 %	25.7 %	74.1 %
D2	0.6256	2.742	0.635	11.6 %	32.2 %	84.8 %
AB	0.2887	1.117	0.105	12.8 %	36.8 %	89.9 %
AC	0.2694	1.041	0.040	14.0 %	41.2 %	93.4 %
AD	0.2581	1.062	0.059	14.8 %	44.2 %	95.1 %
BC	0.3258	1.277	0.217	11.1 %	30.1 %	81.8 %
BD	0.3009	1.246	0.197	12.2 %	34.3 %	87.4 %
CD	0.2850	1.180	0.153	13.0 %	37.6 %	90.6 %

**Basis Std. Dev. = 1.0

Measures Derived From the (X'X)-1 Matrix

Std	Leverage
1	0.4569
2	0.6491
3	0.1032
4	0.6756
5	0.1020
6	0.6358
7	0.1030
8	0.4568
9	0.6998
10	0.5241
11	0.6828
12	0.5747
13	0.4325
14	0.7538
15	0.6805
16	0.6805
17	0.1057
18	0.6067
19	0.2561
20	0.1015
21	0.7021
22	0.1057
23	0.6279
24	0.2747
25	0.6691
26	0.6689
27	0.6778
28	0.7797
29	0.7045
30	0.5084
Average =	0.5000

Maximum Prediction Variance (at a design point) = 0.780
Average Prediction Variance = 0.500

Condition Number of Coefficient Matrix = 14.785

G Efficiency (calculated from the design points) = 64.1 %

Scaled D-optimality Criterion = 2.797

Determinant of (X'X) = 3.497E-16
Trace of (X'X)= 2.386

Correlation Matrix of Regression Coefficients

	Intercept	A	B	C	D	A2	B2
Intercept	1.000						
A	0.014	1.000					
B	0.025	0.127	1.000				
C	0.063	-0.048	0.151	1.000			
D	0.099	0.103	0.078	-0.117	1.000		
A2	-0.147	-0.035	-0.009	0.195	-0.150	1.000	
B2	-0.279	-0.191	-0.292	-0.040	-0.246	-0.091	1.000
C2	-0.098	0.196	0.027	-0.345	0.419	-0.413	-0.134
D2	-0.158	-0.058	0.073	0.085	-0.172	-0.358	-0.184
AB	-0.068	-0.202	-0.138	-0.023	-0.043	0.027	0.224
AC	0.017	-0.078	-0.005	0.054	0.031	-0.031	-0.015
AD	0.048	-0.016	0.017	0.092	-0.076	0.047	-0.025
BC	-0.075	-0.025	-0.136	-0.226	-0.052	-0.141	0.262
BD	0.123	0.018	-0.055	-0.036	-0.111	0.010	-0.251
CD	0.065	0.065	-0.042	0.175	-0.041	0.069	-0.245

	C2	D2	AB	AC	AD	BC	BD
C2	1.000						
D2	-0.416	1.000					
AB	-0.039	-0.040	1.000				
AC	0.001	0.027	0.105	1.000			
AD	-0.201	0.119	-0.086	-0.004	1.000		
BC	0.234	-0.139	0.018	0.070	-0.068	1.000	
BD	-0.156	0.193	-0.066	-0.021	0.123	-0.237	1.000
CD	-0.019	0.044	-0.052	-0.083	0.022	-0.199	0.197

	CD
CD	1.000

Correlation Matrix of Factors [Pearson's r]

	A	B	C	D	A2	B2	C2
A	1.000						
B	-0.072	1.000					
C	0.012	-0.146	1.000				
D	0.007	0.026	0.013	1.000			
A2	-0.029	0.053	0.032	0.075	1.000		
B2	0.069	0.253	0.030	0.219	0.442	1.000	
C2	-0.117	0.005	0.246	-0.188	0.679	0.414	1.000
D2	-0.007	0.010	0.083	0.086	0.718	0.459	0.682
AB	0.156	0.062	0.022	-0.009	-0.068	-0.172	-0.048
AC	0.059	0.017	-0.088	-0.029	0.028	0.070	0.007
AD	-0.003	-0.006	-0.030	-0.008	0.030	0.012	0.117
BC	0.019	0.082	0.130	0.143	-0.013	-0.154	-0.170
BD	-0.005	0.126	0.149	0.127	0.100	0.239	0.128
CD	-0.030	0.144	-0.188	0.093	-0.014	0.177	-0.065

	D2	AB	AC	AD	BC	BD	CD
D2	1.000						
AB	-0.047	1.000					
AC	-0.002	-0.106	1.000				
AD	0.005	0.080	-0.003	1.000			
BC	-0.026	0.063	-0.084	-0.006	1.000		
BD	0.027	0.017	-0.007	-0.081	0.164	1.000	
CD	0.001	-0.007	0.088	0.007	0.105	-0.115	1.000

Table C.4 – Complete Model Fit Summary of Model to Experimental Data

Response: Fe(II) regeneration rate Transform: Natural log Constant: 0
*** WARNING: The Cubic Model is Aliased! ***

Sequential Model Sum of Squares

Source	Sum of Squares	DF	Mean Square	F Value	Prob > F	
Mean	499.584	1	499.584			
Linear	4.967	4	1.242	3.588	0.0191	
2FI	1.894	6	0.316	0.888	0.5231	
Quadratic	5.033	4	1.258	10.943	0.0002	Suggested
Cubic	1.725	15	0.115			Aliased
Residual	0.000	0				
Total	513.204	30	17.107			

"Sequential Model Sum of Squares": Select the highest order polynomial where the additional terms are significant and the model is not aliased.

Model Summary Statistics

Source	Std. Dev.	R-Squared	Adjusted R-Squared	Predicted R-Squared	PRESS	
Linear	0.5883	0.3647	0.2631	0.0511	12.9236	
2FI	0.5964	0.5038	0.2427	-0.6618	22.6331	
Quadratic	0.3391	0.8734	0.7552	0.5788	5.7361	Suggested
Cubic					+	Aliased

+ Case(s) with leverage of 1.0000: PRESS statistic not defined

Table C.5 – Analysis of Variance (ANOVA) for Model and Experimental Data

ANOVA for Response Surface Reduced Quadratic Model
Analysis of variance table [Partial sum of squares]

Source	Sum of Squares	DF	Mean Square	F Value	Prob > F	
Model	11.41	5	2.28	24.76	< 0.0001	significant
B	2.1900	1	2.19000	23.82000	< 0.0001	
D	4.8900	1	4.89000	53.07000	< 0.0001	
C2	5.2000	1	5.20000	56.40000	< 0.0001	
AC	0.7700	1	0.77000	8.37000	0.008	
BD	0.8600	1	0.86000	9.32000	0.0055	
Residual	2.2100	24	0.09200			
Cor Total	13.6200	29				

The Model F-value of 24.76 implies the model is significant. There is only a 0.01% chance that a "Model F-Value" this large could occur due to noise.

Values of "Prob > F" less than 0.0500 indicate model terms are significant.
In this case B, D, C^2, AC, BD are significant model terms.
Values greater than 0.1000 indicate the model terms are not significant.
If there are many insignificant model terms (not counting those required to support hierarchy), model reduction may improve your model.

Std. Dev.	0.3	R-Squared	0.8376
Mean	-4.08	Adj R-Squared	0.8038
C.V.	-7.44	Pred R-Squared	0.7694
PRESS	3.14	Adeq Precision	17.792

The "Pred R-Squared" of 0.7694 is in reasonable agreement with the "Adj R-Squared" of 0.8038.

Adeq Precision measures the signal to noise ratio. A ratio greater than 4 is desirable. Your ratio of 17.792 indicates an adequate signal. This model can be used to navigate the design space.

Coefficient Factor	Standard Estimate	95% CI DF	95% CI Error	Low	High	VIF
Intercept	-3.64	1	0.087	-3.82	-3.46	
B-Fe3+ concentration	0.47	1	0.097	0.27	0.67	1.02
D-carbon particle size	-0.54	1	0.074	-0.69	-0.38	1.07
C2	-1.24	1	0.17	-1.58	-0.9	1.06
AC	-0.27	1	0.092	-0.46	-0.077	1
BD	0.33	1	0.11	0.11	0.55	1.06

Final Equation in Terms of Coded Factors:

Ln(Fe(II) regeneration rate) =

-3.64
0.47 * B
-0.54 * D
-1.24 * C2
-0.27 * A * C
0.33 * B * D

Diagnostics Case Statistics

Standard Order	Actual Value	Predicted Value	Residual	Leverage	Student Residual	Cook's Distance	Outlier t	Run Order
1	-5.81	-5.49	-0.32	0.298	-1.254	0.111	-1.27	26
2	-4	-4.4	0.4	0.141	1.42	0.055	1.453	23
3	-4.27	-4.16	-0.11	0.352	-0.443	0.018	-0.436	24
4	-4.18	-3.91	-0.27	0.173	-0.982	0.034	-0.981	21
5	-4.5500	-4.5	-0.059	0.317	-0.235	0.004	-0.23	6
6	-4.5100	-4.71	0.21	0.386	0.872	0.08	0.868	9
7	-5.1400	-5.31	0.17	0.225	0.618	0.019	0.61	1
8	-5.2000	-5.18	-0.015	0.274	-0.058	0	-0.056	17
9	-3.5700	-3.86	0.29	0.308	1.142	0.097	1.15	12
10	-3.7100	-3.67	-0.032	0.249	-0.122	0.001	-0.119	11
11	-5.3800	-5.17	-0.21	0.276	-0.816	0.042	-0.81	5
12	-3.8000	-3.56	-0.23	0.081	-0.798	0.009	-0.792	15
13	-3.5400	-3.59	0.051	0.081	0.174	0	0.17	27
14	-3.5700	-3.55	-0.015	0.081	-0.05	0	-0.049	2
15	-4.4400	-4.1	-0.34	0.034	-1.147	0.008	-1.155	14
16	-3.3100	-3.23	-0.082	0.139	-0.291	0.002	-0.285	18
17	-4.2100	-3.58	-0.63	0.085	-2.183	0.074	-2.388	25
18	-4.1900	-3.99	-0.2	0.259	-0.782	0.036	-0.775	8
19	-4.6000	-4.36	-0.24	0.269	-0.911	0.051	-0.907	29
20	-3.82	-3.83	3.01E-03	0.253	0.011	0	0.011	22
21	-3.42	-3.65	0.23	0.075	0.793	0.009	0.787	19
22	-3.6	-3.47	-0.13	0.083	-0.444	0.003	-0.436	10
23	-4.66	-4.45	-0.21	0.246	-0.807	0.035	-0.801	13
24	-3.39000	-3.51	0.12	0.082	0.407	0.002	0.4	7
25	-3.00000	-3.6	0.6	0.066	2.053	0.049	2.214	4
26	-3.79000	-4.06	0.27	0.2	0.993	0.041	0.993	3
27	-3.67000	-3.63	-0.039	0.318	-0.156	0.002	-0.153	30
28	-4.25000	-4.48	0.24	0.440 #	1.036	0.14	1.038	28
29	-3.73000	-4.33	0.6	0.056	2.033	0.041	2.187	16
30	-3.11000	-3.08	-0.03	0.156	-0.109	0	-0.106	20

Obs with Leverage > 2.00 *(average leverage)

Vita

Emily Allyn Sarver is the daughter of Stephen and Pat Sarver, and was born April 24, 1981 in Richmond, VA. She grew up in Smithfield, VA, and moved back to Richmond in 1997, where she graduated from Monacan High School in 1999. She received her Bachelor of Science degree in Mining and Minerals Engineering from Virginia Polytechnic Institute and State University (Virginia Tech) in May of 2004.

Upon being awarded a National Science Foundation Graduate Research Fellowship in 2004, Emily chose to stay at Virginia Tech to pursue a Master of Science degree, also in Mining and Minerals Engineering. Her research work included a joint project with the Phelps Dodge Process Technology Center in Morenci, AZ.

Emily's remaining NSF tenure will be used in pursuit of a Doctorate degree in Materials Science and Engineering.